US 20110237911A1

(19) United States

(12) Patent Application Publication

Lamego et al.

(10) Pub. No.: US 2011/0237911 A1

(43) Pub. Date: Sep. 29, 2011

(54) **MULTIPLE-WAVELENGTH PHYSIOLOGICAL MONITOR**

(75) Inventors: **Marcelo M. Lamego**, Coto De Caza, CA (US); **Mohamed Diab**, Ladera Ranch, CA (US); **Walter M. Weber**, Laguna Hills, CA (US); **Ammar Al-Ali**, Tustin, CA (US); **Massi Joe E. Kiani**, Laguna Niguel, CA (US)

(73) Assignee: **MASIMO LABORATORIES, INC.**, Irvine, CA (US)

(21) Appl. No.: **13/073,778**

(22) Filed: **Mar. 28, 2011**

Related U.S. Application Data

(63) Continuation-in-part of application No. 12/045,309, filed on Mar. 10, 2008, which is a continuation of application No. 11/139,291, filed on May 27, 2005, now Pat. No. 7,343,186.

(60) Provisional application No. 61/318,735, filed on Mar. 29, 2010, provisional application No. 60/586,069, filed on Jul. 7, 2004.

Publication Classification

(51) **Int. Cl.**
A61B 5/1455 (2006.01)

(52) **U.S. Cl.** **600/323**

(57) **ABSTRACT**

A physiological monitor for determining blood oxygen saturation of a medical patient includes a sensor, a signal processor and a display. The sensor includes at least three light emitting diodes. Each light emitting diode is adapted to emit light of a different wavelength. The sensor also includes a detector, where the detector is adapted to receive light from the three light emitting diodes after being attenuated by tissue. The detector generates an output signal based at least in part upon the received light. The signal processor determines blood oxygen saturation based at least upon the output signal, and the display provides an indication of the blood oxygen saturation.

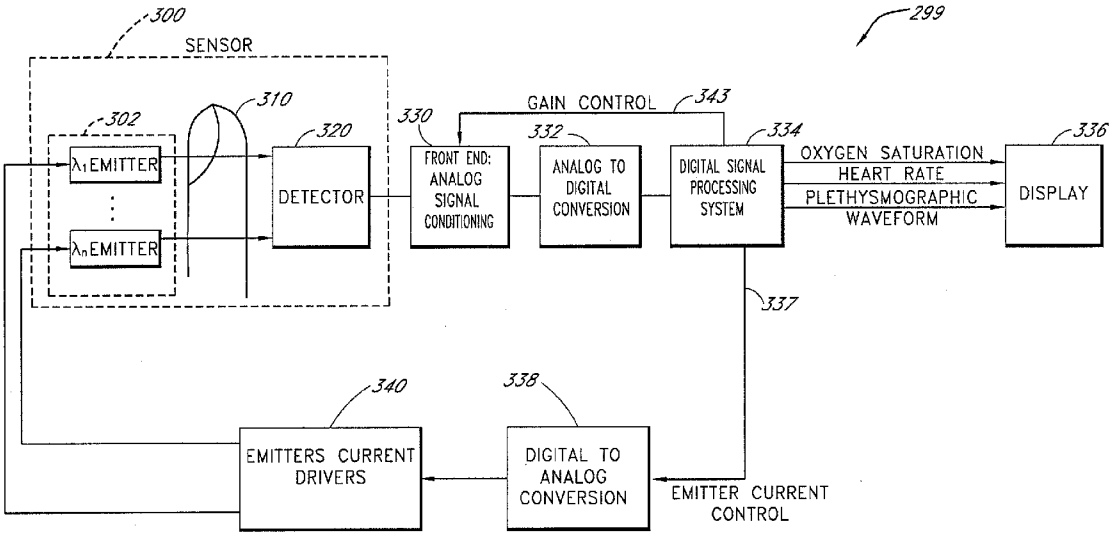

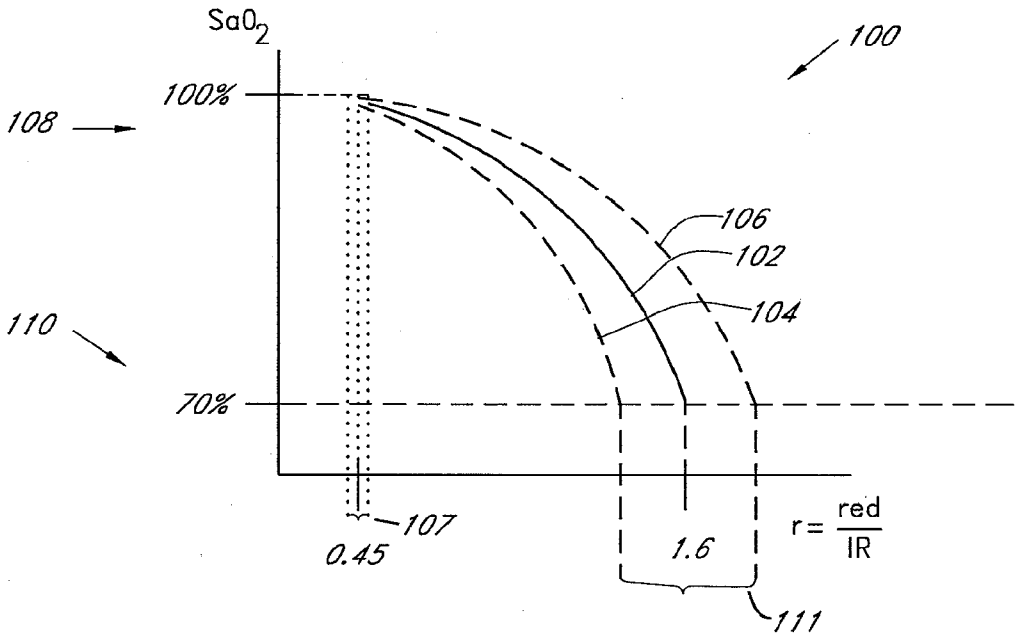

FIG. 1 (Prior Art)

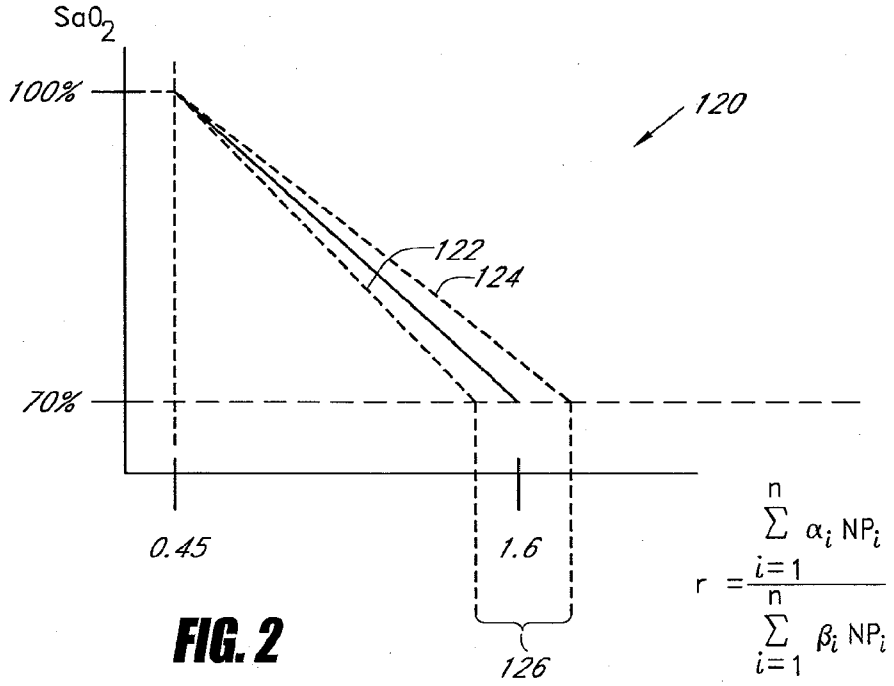

FIG. 2

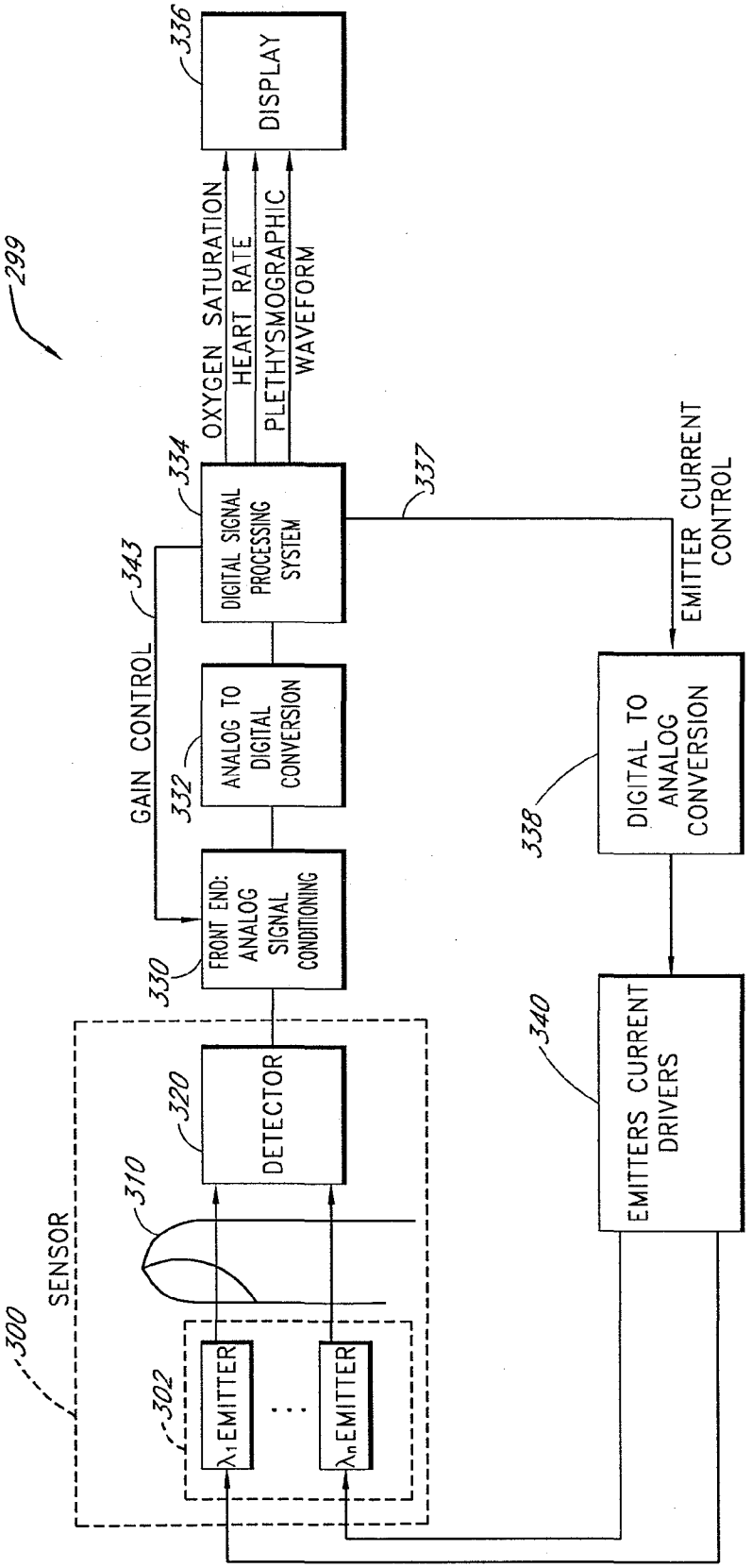
299
336
DISPLAY
OXYGEN SATURATION
HEART RATE
PLETHYSMOGRAPHIC WAVEFORM
334
DIGITAL SIGNAL PROCESSING SYSTEM
337
EMITTER CURRENT CONTROL
343
GAIN CONTROL
332
ANALOG TO DIGITAL CONVERSION
338
DIGITAL TO ANALOG CONVERSION
330
FRONT END: ANALOG SIGNAL CONDITIONING
340
EMITTERS CURRENT DRIVERS
320
DETECTOR
310
SENSOR
300
302
λ1 EMITTER
λn EMITTER

FIG. 3

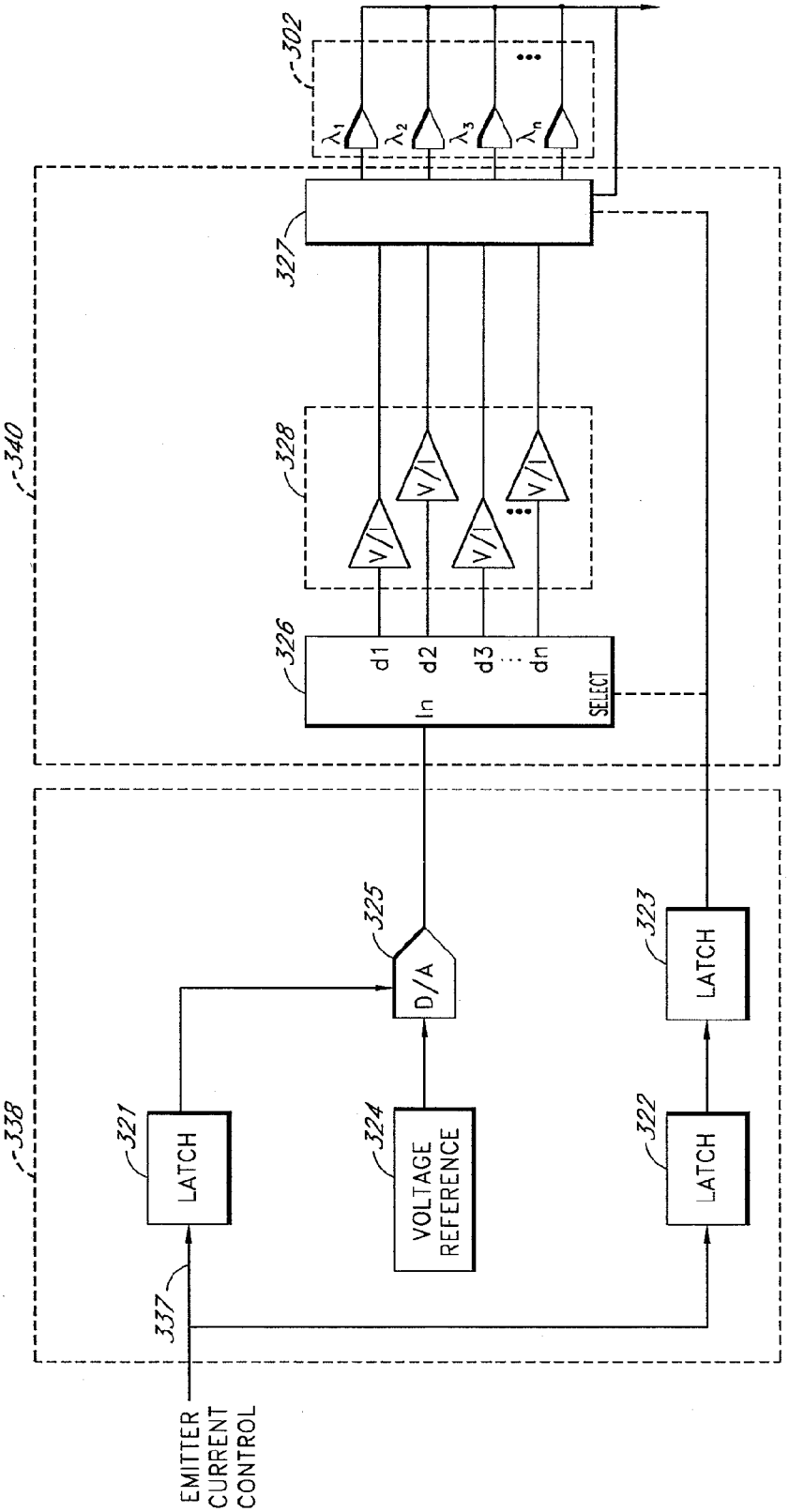
302
λ1
λ2
λ3
λn
327
340
328
V/I
326
d1
d2
d3
dn
In
SELECT
325
D/A
323
LATCH
338
321
LATCH
324
VOLTAGE REFERENCE
322
LATCH
337
EMITTER CURRENT CONTROL

FIG. 3A

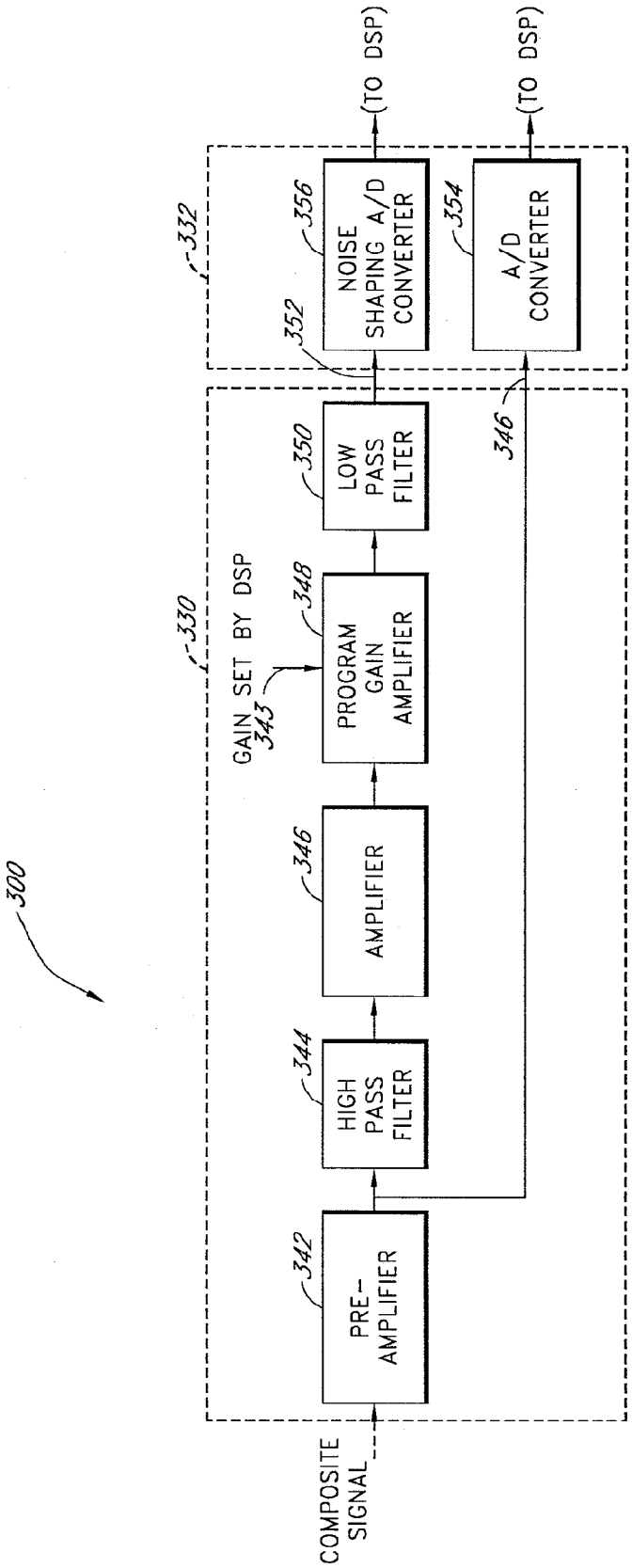
300
COMPOSITE SIGNAL
PRE-AMPLIFIER
342
HIGH PASS FILTER
344
AMPLIFIER
346
GAIN SET BY DSP
343
PROGRAM GAIN AMPLIFIER
348
LOW PASS FILTER
350
330
352
NOISE SHAPING A/D CONVERTER
356
332
A/D CONVERTER
354
346
(TO DSP)
(TO DSP)

FIG. 4

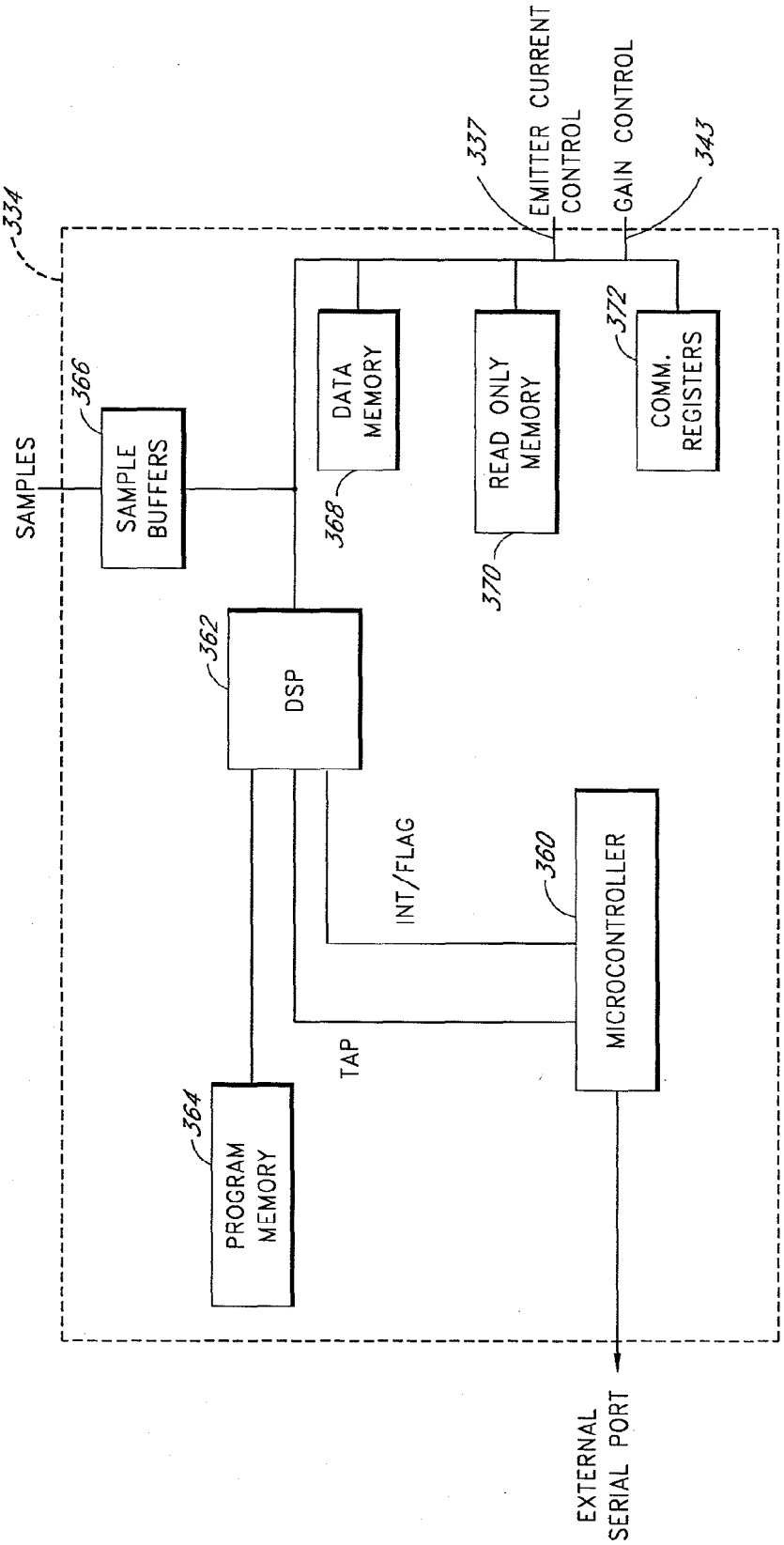
334
SAMPLES
366
SAMPLE BUFFERS
DATA MEMORY
368
READ ONLY MEMORY
370
COMM. REGISTERS
372
EMITTER CURRENT CONTROL
337
GAIN CONTROL
343
DSP
362
INT/FLAG
MICROCONTROLLER
360
TAP
PROGRAM MEMORY
364
EXTERNAL SERIAL PORT

FIG. 5

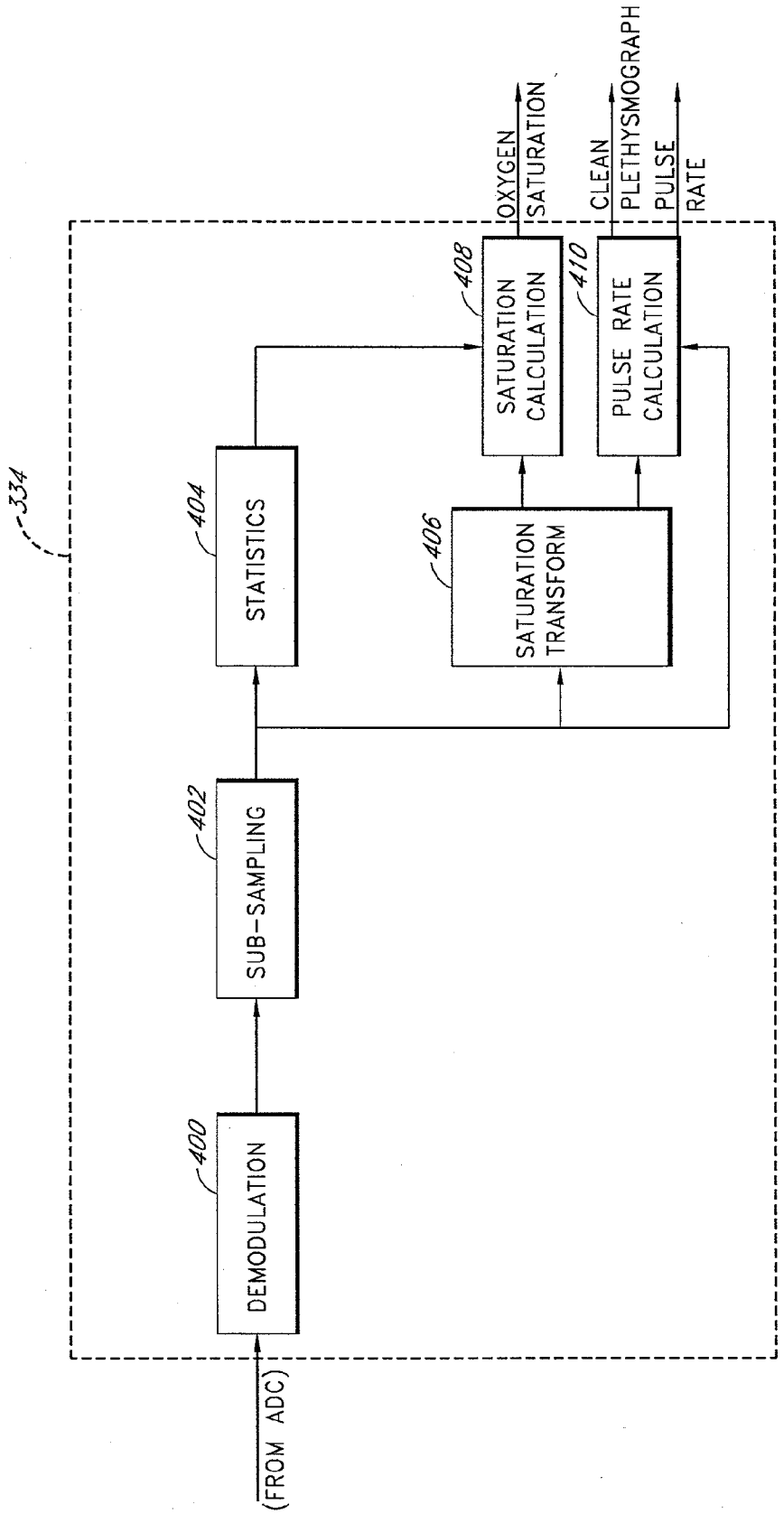
334
(FROM ADC)
400
DEMODULATION
402
SUB-SAMPLING
404
STATISTICS
406
SATURATION TRANSFORM
408
SATURATION CALCULATION
410
PULSE RATE CALCULATION
OXYGEN SATURATION
CLEAN PLETHYSMOGRAPH
PULSE RATE

FIG. 6

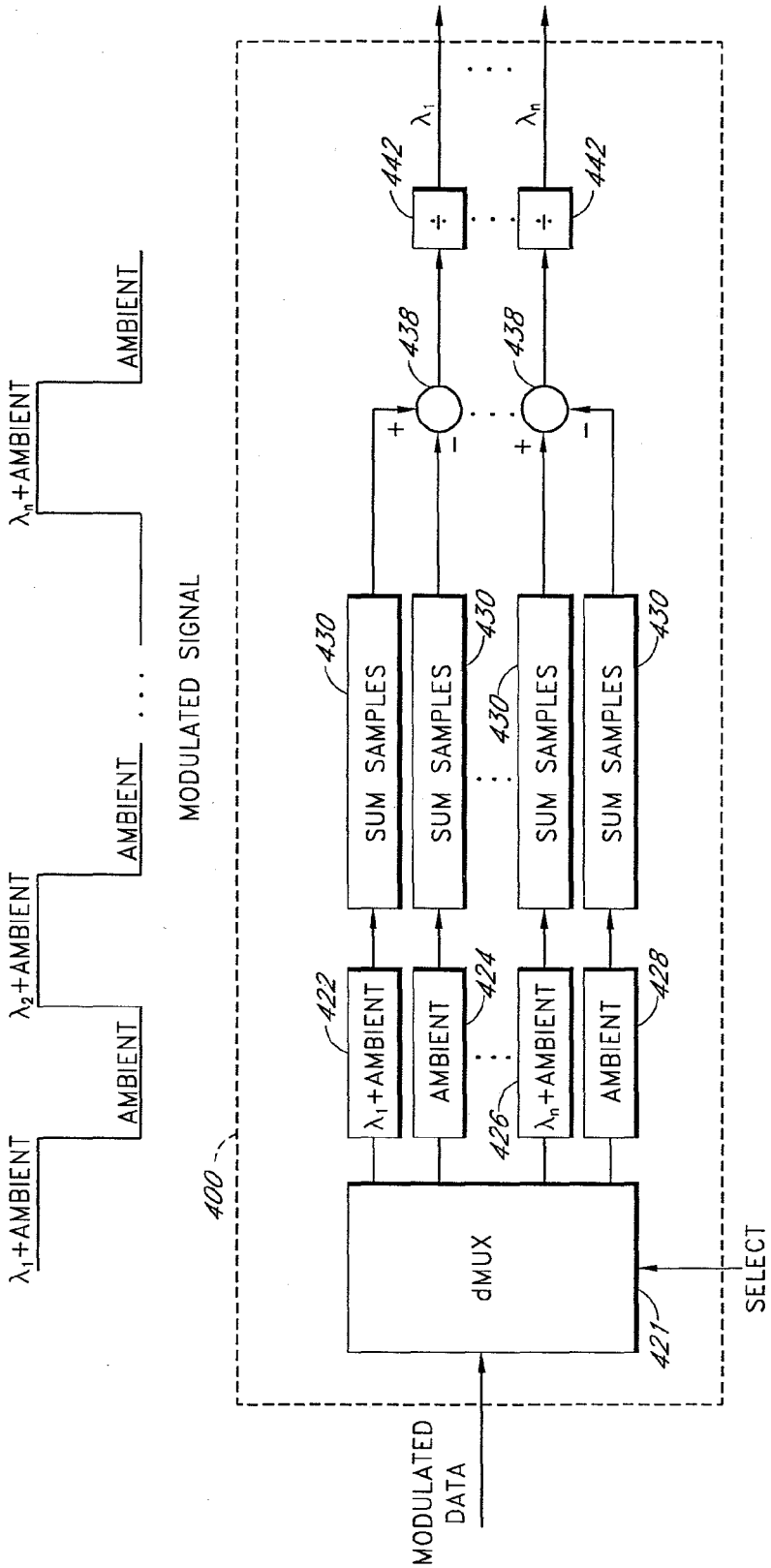
λ1+AMBIENT
AMBIENT
λ2+AMBIENT
AMBIENT
λn+AMBIENT
AMBIENT
MODULATED SIGNAL
400
MODULATED DATA
dMUX
421
SELECT
λ1+AMBIENT
422
AMBIENT
424
λn+AMBIENT
426
AMBIENT
428
SUM SAMPLES
430
SUM SAMPLES
430
SUM SAMPLES
430
SUM SAMPLES
430
+
−
+
−
438
438
÷
÷
442
442
λ1
λn

FIG. 7

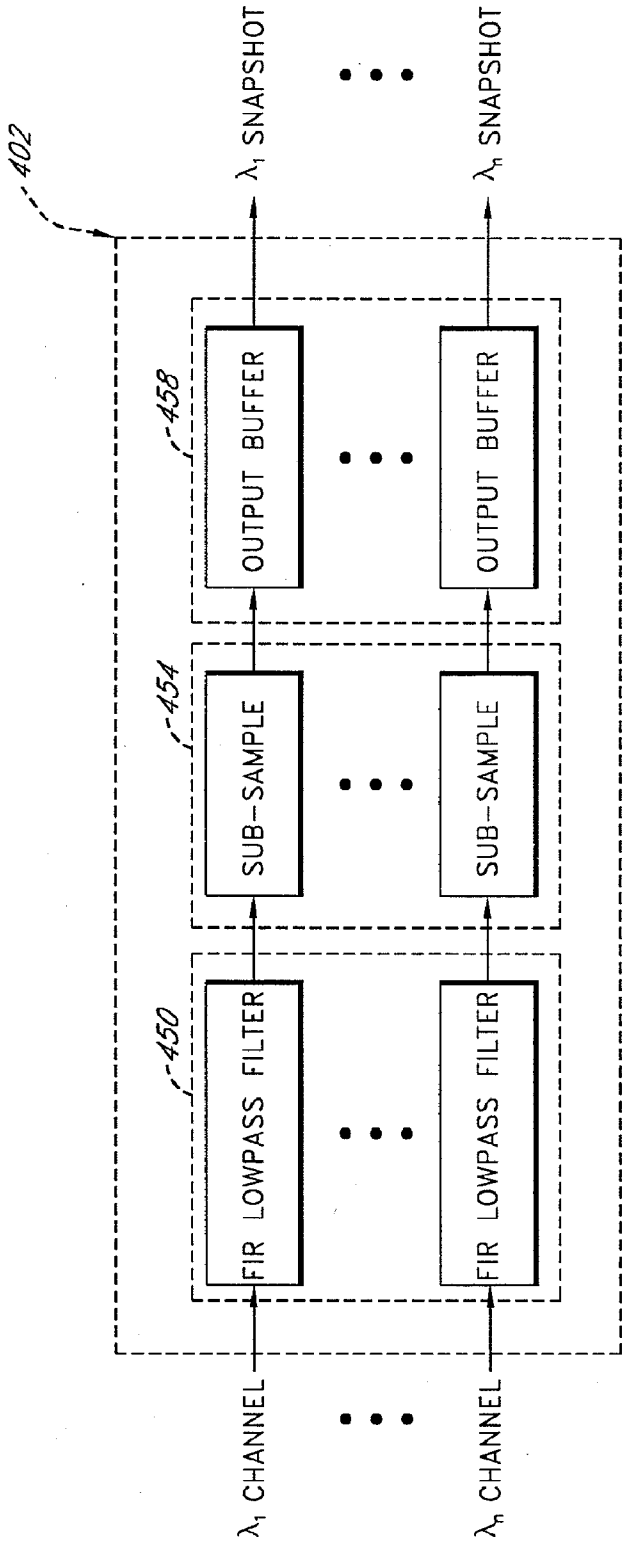
402
450
454
458
λ_1 CHANNEL
λ_n CHANNEL
FIR LOWPASS FILTER
FIR LOWPASS FILTER
SUB-SAMPLE
SUB-SAMPLE
OUTPUT BUFFER
OUTPUT BUFFER
λ_1 SNAPSHOT
λ_n SNAPSHOT

FIG. 8

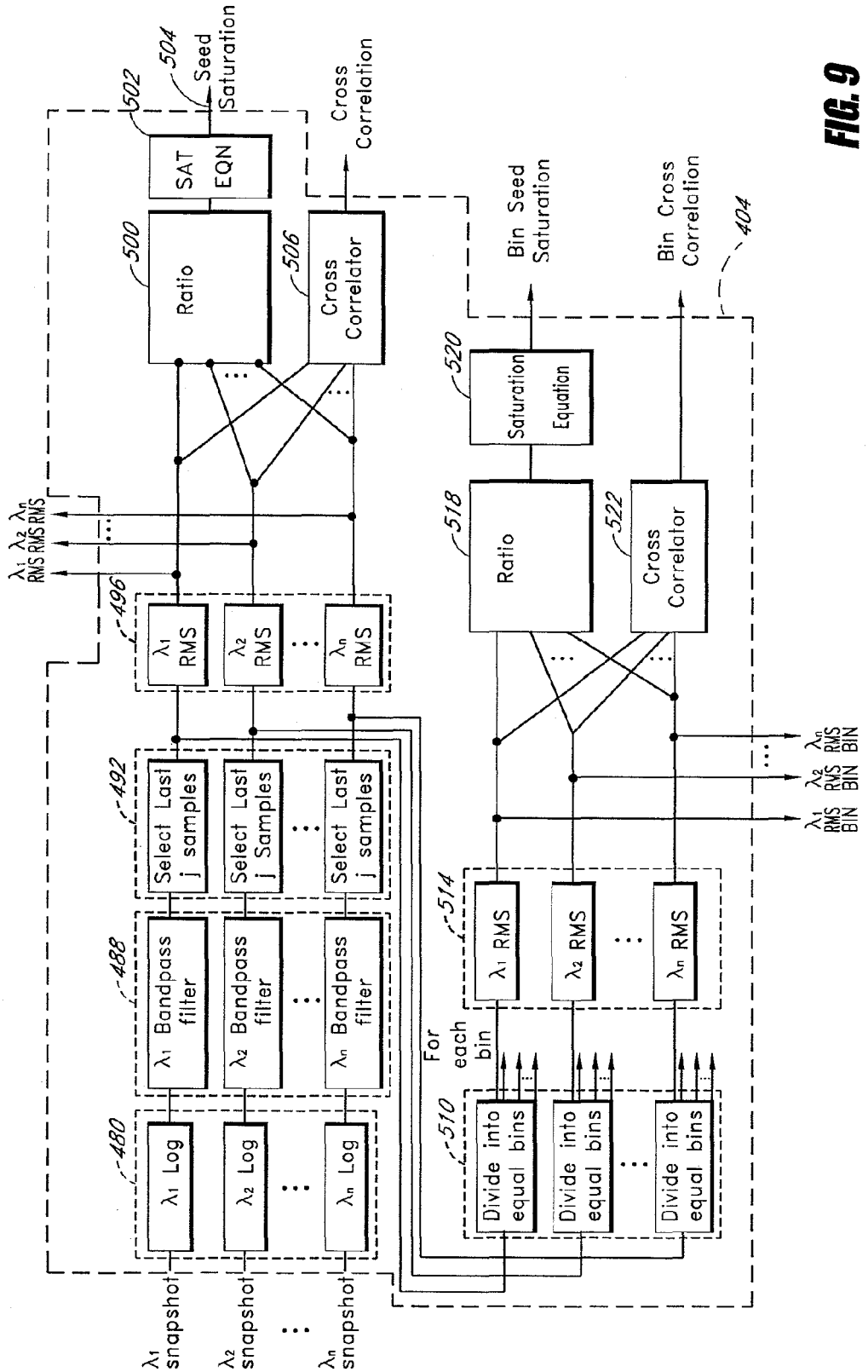
λ1 snapshot
λ2 snapshot
λn snapshot
480
λ1 Log
λ2 Log
λn Log
488
λ1 Bandpass filter
λ2 Bandpass filter
λn Bandpass filter
492
Select Last j samples
Select Last j Samples
Select Last j samples
496
λ1 RMS
λ2 RMS
λn RMS
λ1 RMS RMS
λ2 RMS RMS
λn RMS RMS
500
Ratio
502
SAT EQN
504
Seed Saturation
506
Cross Correlator
Cross Correlation
For each bin
510
Divide into equal bins
Divide into equal bins
Divide into equal bins
514
λ1 RMS
λ2 RMS
λn RMS
λ1 RMS BIN
λ2 RMS BIN
λn RMS BIN
518
Ratio
520
Saturation Equation
522
Cross Correlator
Bin Seed Saturation
Bin Cross Correlation
404

FIG. 9

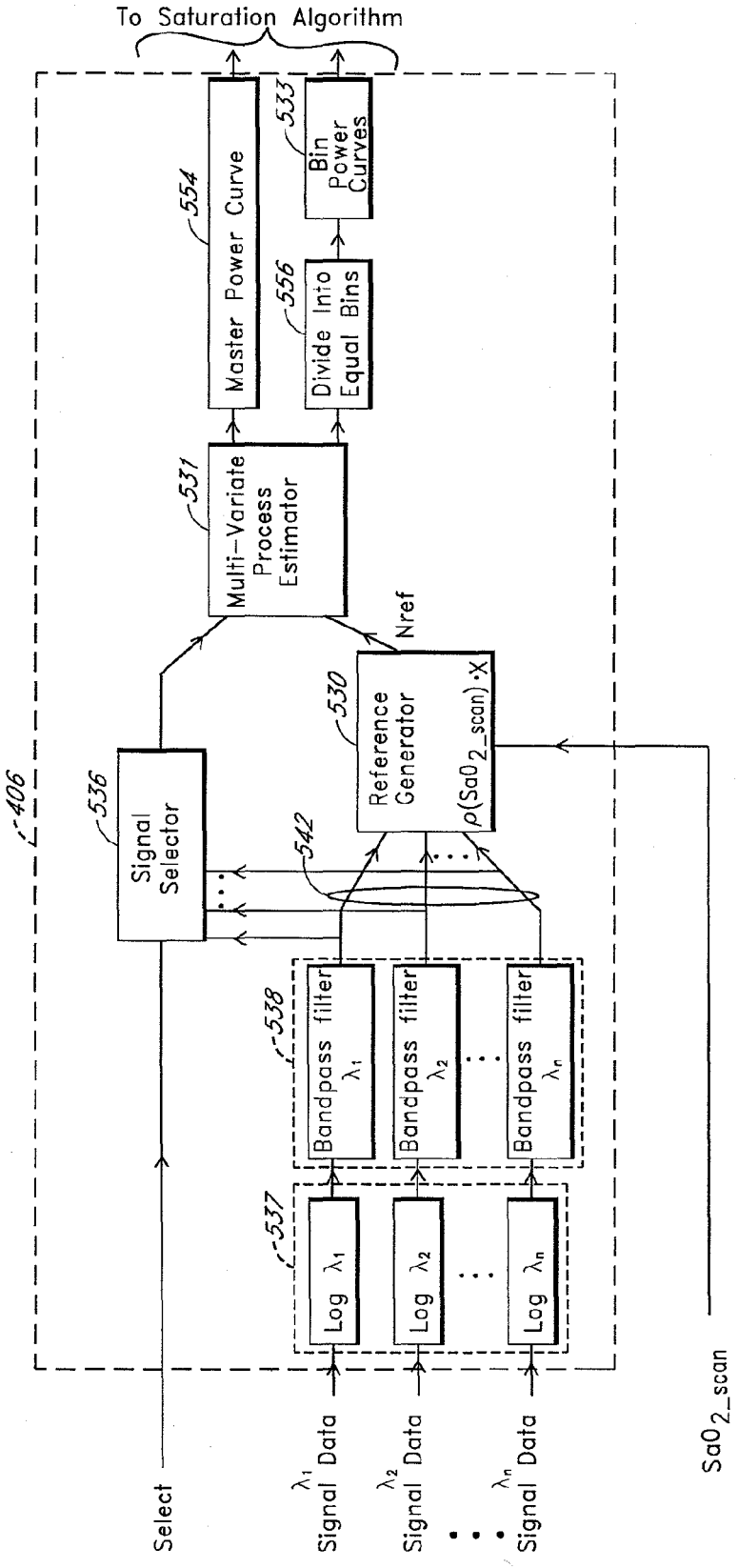
To Saturation Algorithm
406
536
Signal Selector
531
Multi-Variate Process Estimator
554
Master Power Curve
533
Bin Power Curves
556
Divide Into Equal Bins
530
Reference Generator
ρ(SaO2_scan)·X
Nref
542
538
Bandpass filter λ1
Bandpass filter λ2
Bandpass filter λn
537
Log λ1
Log λ2
Log λn
Select
λ1 Signal Data
λ2 Signal Data
λn Signal Data
SaO2_scan

FIG. 10

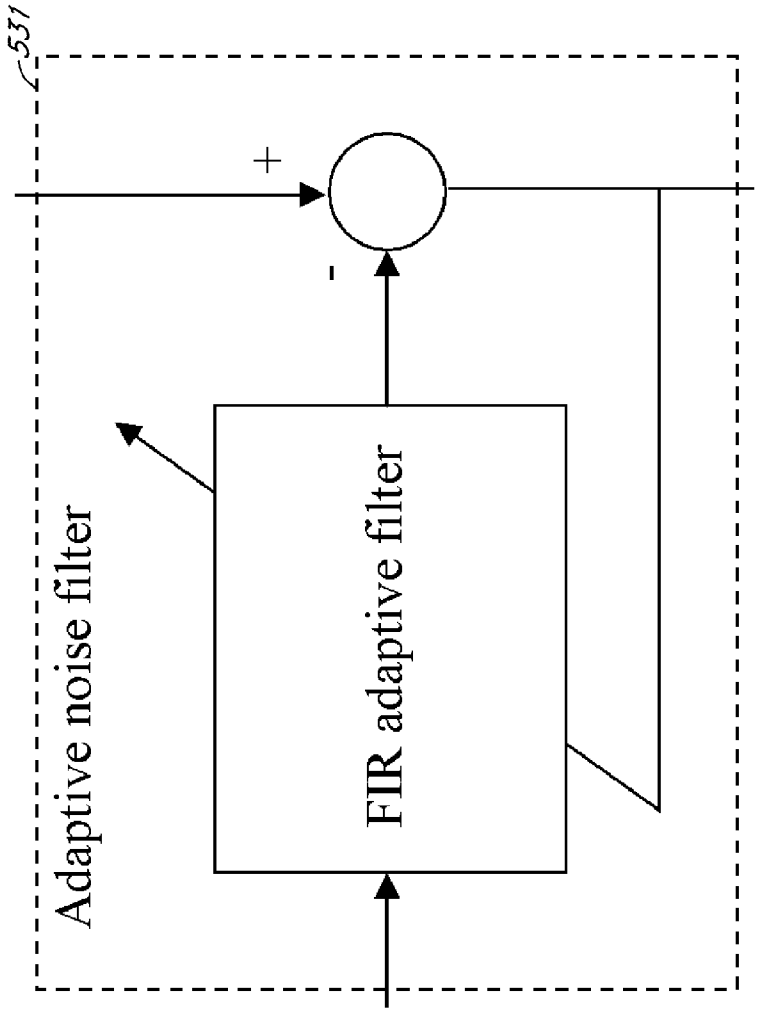

FIG. 10A

FIG. 11

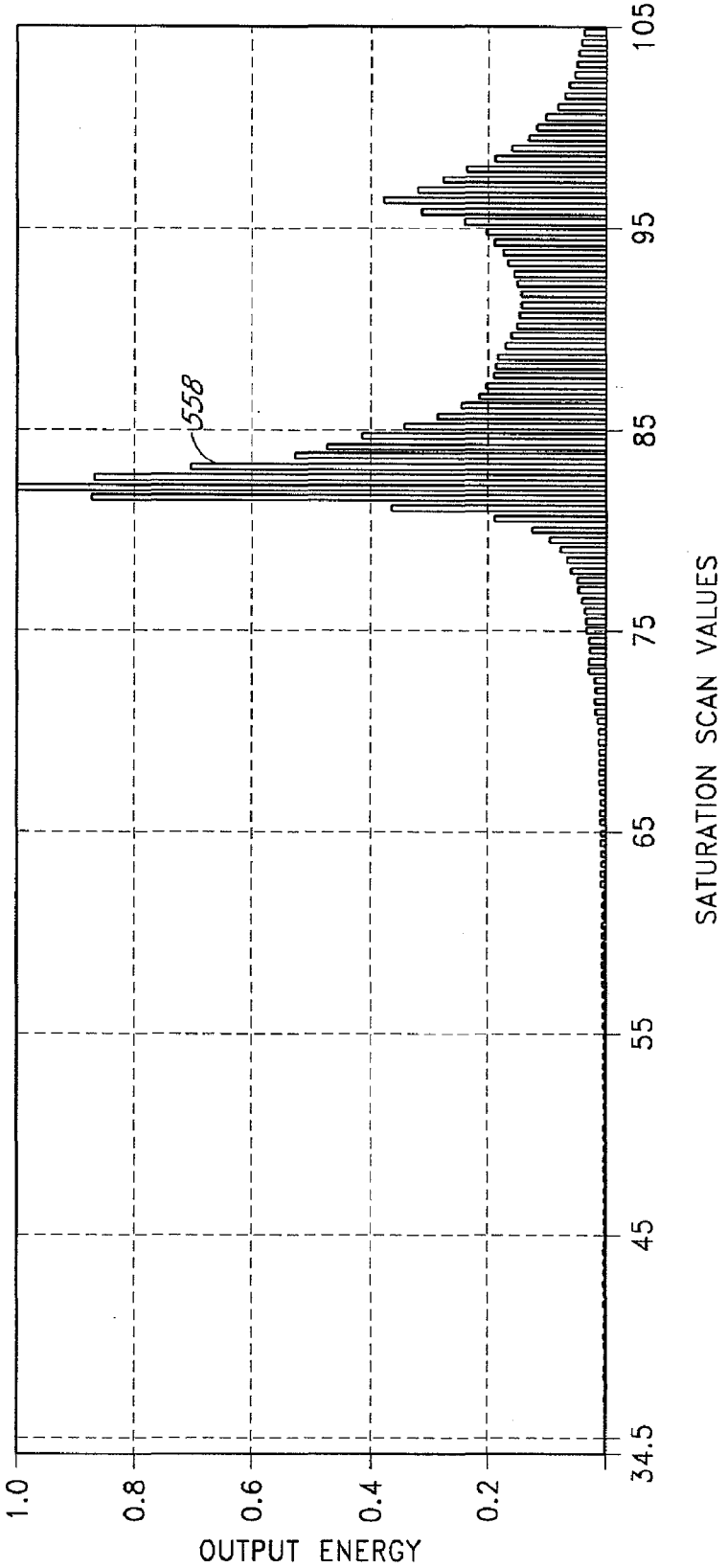
558
1.0
0.8
0.6
0.4
0.2
OUTPUT ENERGY
34.5
45
55
65
75
85
95
105
SATURATION SCAN VALUES

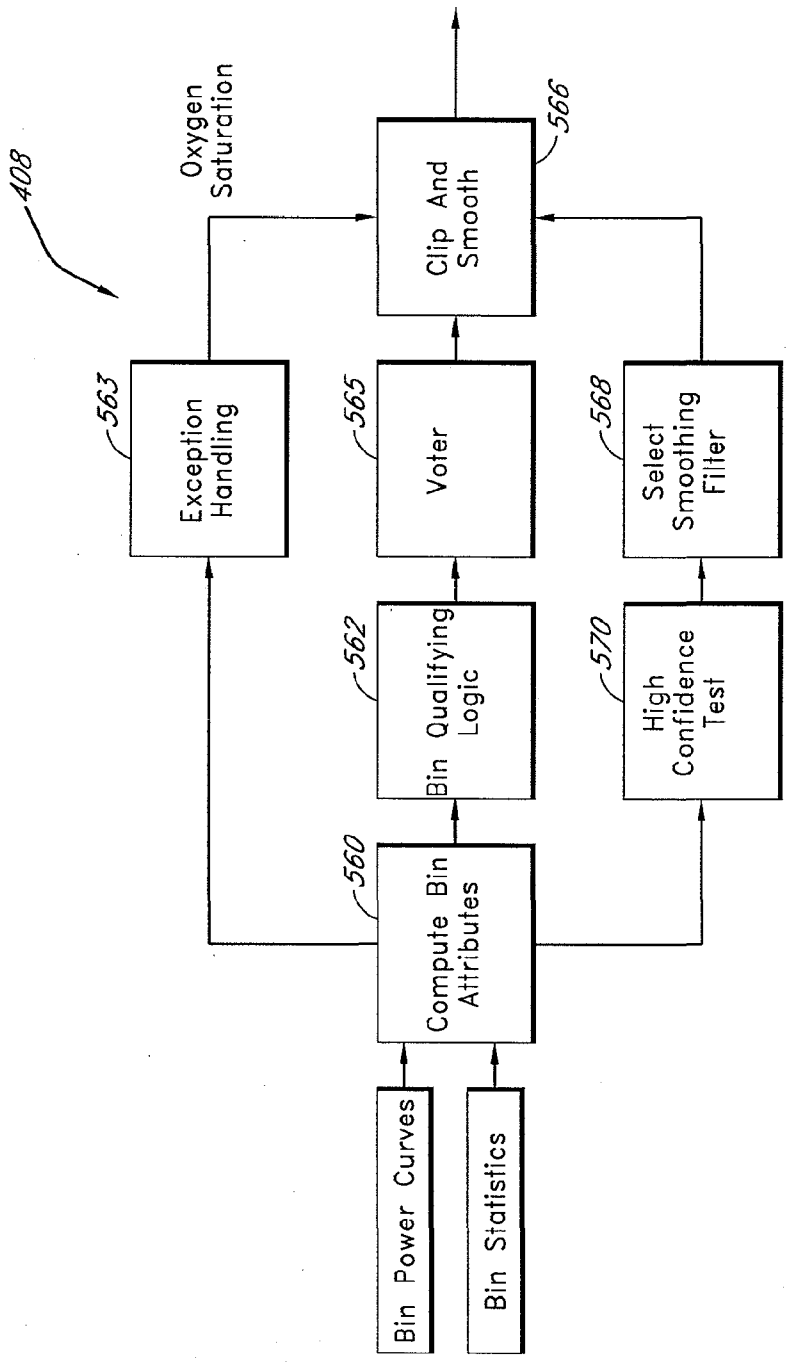
408
Bin Power Curves
Bin Statistics
560
Compute Bin Attributes
562
Bin Qualifying Logic
563
Exception Handling
Oxygen Saturation
565
Voter
570
High Confidence Test
568
Select Smoothing Filter
566
Clip And Smooth

FIG. 12

MULTIPLE-WAVELENGTH PHYSIOLOGICAL MONITOR

RELATED APPLICATIONS

[0001] This application claims priority from U.S. Provisional No. 61/318,735, filed Mar. 29, 2010 and is a continuation-in-part of U.S. application Ser. No. 12/045,309, filed Mar. 10, 2008, which is a continuation of U.S. application Ser. No. 11/139,291, filed May 27, 2005, now U.S. Pat. No. 7,343,186, which claims priority from U.S. Provisional No. 60/586,069, filed Jul. 7, 2004. All of the foregoing are expressly incorporated by reference herein.

BACKGROUND

[0002] 1. Field

[0003] The present invention relates to the field of signal processing. More specifically, the present invention relates to the processing of measured signals which contain a primary signal portion and a secondary signal portion for the removal or derivation of either signal portion. The present invention is especially useful for physiological monitoring systems, including blood oxygen saturation measurement systems and oximeters.

[0004] 2. Description of the Related Art

[0005] Blood oxygen saturation measurement systems, oximeters, and physiological monitors of the prior art generally utilize two different wavelengths of light to determine a patient's blood oxygen saturation level. In general, such systems provide two wavelengths of light to a target location on a patient's body. The systems then measure at least one signal indicative of the transmission or reflection of the two light wavelengths with respect to the tissue at the target location.

[0006] One such physiological monitor is taught by Diab et al. in U.S. Pat. No. 5,632,272, incorporated by reference herein in its entirety. One embodiment of Diab's physiological monitor provides light having a red wavelength and light having an infrared wavelength to one side of a patient's finger. A detector on the opposite side of the patient's finger measures the red and infrared wavelength light transmitted through the patient's finger and generates a measurement signal. A processor analyzes the measurement signal to determine red and infrared component signals. Possible saturation values are input to a saturation equation module which provides reference coefficients. The red or infrared component signal is processed with the reference coefficients to yield reference signal vectors.

[0007] The reference signal vectors and the red or infrared component signal are processed by a correlation canceller to generate output vectors. The output vectors are input into a master power curve module, which provides a blood oxygen saturation value for each possible saturation value input to the saturation equation module. The patient's blood oxygen saturation is determined based upon the power curve module output.

BRIEF DESCRIPTION OF THE DRAWINGS

[0008] FIG. **1** illustrates an arterial blood oxygen saturation curve in accordance with the prior art.

[0009] FIG. **2** illustrates an arterial blood oxygen saturation curve of a multi-wavelength physiological monitor in accordance with one embodiment of the present invention.

[0010] FIG. **3** is an example of a physiological monitor in accordance with one embodiment of the present invention.

[0011] FIG. **3**A illustrates one embodiment of the low noise emitter current driver of the physiological monitor of FIG. **3**.

[0012] FIG. **4** illustrates one embodiment of the front end analog signal conditioning circuitry and the analog to digital conversion circuitry of the physiological monitor of FIG. **3**.

[0013] FIG. **5** illustrates one embodiment of the digital signal processing circuitry of FIG. **3**.

[0014] FIG. **6** illustrates one embodiment of additional operations performed by the digital signal processing circuitry of FIG. **3**.

[0015] FIG. **7** illustrates one embodiment of the demodulation module of FIG. **6**.

[0016] FIG. **8** illustrates one embodiment of the sub-sampling module of FIG. **6**.

[0017] FIG. **9** illustrates one embodiment of the statistics module of FIG. **6**.

[0018] FIG. **10** illustrates a block diagram of the operations of one embodiment of the saturation transform module of FIG. **6**.

[0019] FIG. **10**A illustrates an adaptive noise filter that may be used as the multi-variate process estimator of FIG. **10**.

[0020] FIG. **11** illustrates a saturation transform curve in accordance with one embodiment of the present invention.

[0021] FIG. **12** illustrates a block diagram of the operation of one embodiment of the saturation calculation module of FIG. **6**.

DETAILED DESCRIPTION

[0022] Spectroscopy is a common technique for measuring the concentration of organic and some inorganic constituents of a solution. The theoretical basis of this technique is the Beer-Lambert law, which states that the concentration c_i of an absorbent in solution can be determined by the intensity of light transmitted through the solution, knowing the path-length d_λ, the intensity of the incident light $I_{0,\lambda}$, and the extinction coefficient $\epsilon_{i,\lambda}$ at a particular wavelength λ. In generalized form, the Beer-Lambert law is expressed as:

$$I_\lambda = I_{0,\lambda} e^{-d_\lambda \cdot \mu_{0,\lambda}} \tag{1}$$

$$\mu_{0,\lambda} = \sum_{i=1}^{n} \varepsilon_{i,\lambda} \cdot c_i \tag{2}$$

[0023] where $\mu_{0,\lambda}$ is the bulk absorption coefficient and represents the probability of absorption per unit length. The minimum number of discrete wavelengths that may be required to solve Equations 1 and 2 is at least the number of significant absorbers that are present in the solution. Least squares or other estimation techniques can be used to approximate a solution to these equations for underdetermined or overdetermined systems. The system of equations is underdetermined if there are fewer equations or wavelengths than unknowns or significant absorbers (e.g., blood constituents). Conversely, the system is overdetermined if there are more equations than unknowns.

[0024] A practical application of this technique is pulse oximetry, which utilizes a noninvasive sensor to measure blood oxygen saturation (SpO_2) and pulse rate. A multi-wavelength physiological monitor in accordance with one embodiment determines blood oxygen saturation by propagating multi-wavelength energy through a medium, such as a portion of a patient's body where blood flows close to the

body surface. For example, in one embodiment, energy is propagated through an ear lobe, a digit (such as a finger or toe), a forehead, or a scalp (such as a fetus's scalp). An attenuated signal is measured after energy propagation through, or reflection from the medium. The physiological monitor determines the saturation of oxygenated blood in the patient based at least in part upon the measured signal.

[0025] It is well known by those of skill in the art that freshly oxygenated blood is pumped at high pressure from the heart into the arteries for use by the body. The volume of blood in the arteries varies with the heartbeat. This variation gives rise to a variation in energy absorption at the heartbeat rate, or the pulse.

[0026] Oxygen depleted, or deoxygenated, blood is returned to the heart through the veins with unused oxygenated blood. Unlike the arteries, the volume of blood in the veins varies with the rate of breathing, which is typically much slower than the heartbeat. Since the blood pressure in the veins is typically much lower than that of the arteries, the volume of blood in the veins varies in response to motion, such as a patient raising or lowering her arm. Changes in blood volume within the veins cause changes in vein thicknesses. Therefore, when there is no motion induced variation in the thickness of the veins, venous blood causes a low frequency variation in energy absorption, which is related to the rate of breathing. However, when erratic, motion-induced variations in the thickness of the veins occur, the low frequency variation in absorption is coupled with an erratic variation in energy absorption due to the erratic motion.

[0027] In one embodiment, absorption measurements are based upon the transmission of energy through a medium. In one embodiment, multiple light emitting diodes (LEDs) are positioned on one side of a portion of the body where blood flows close to the body's surface, such as a finger, and a photodetector is positioned on the opposite side of the surface. In another embodiment one or more such LEDs emit light of different wavelengths. In one embodiment, one LED emits a visible wavelength, such as red, and the other LED emits an infrared wavelength. However, one skilled in the art will realize that other wavelength combinations could be used.

[0028] The finger comprises skin, tissue, muscle, both arterial blood and venous blood, fat, etc., each of which absorbs light energy differently due to different absorption coefficients, different concentrations, different thicknesses, and changing optical pathlengths. When the patient is not moving, absorption is substantially constant except for variations due to the flow of blood through the skin, tissue, muscle, etc. A constant attenuation can be determined and subtracted from the measured signal via traditional filtering techniques. However, when the patient moves, perturbations such as changing optical pathlengths occur. Such perturbations may be due to movement of background fluids, (such as venous blood, which has a different saturation than arterial blood). Therefore, the measured signal becomes erratic. Erratic, motion-induced noise typically cannot be predetermined and subtracted from the measured signal via traditional filtering techniques. Thus, determining the oxygen saturation of arterial blood and venous in erratic, motion-induced noise environments, blood becomes more difficult.

[0029] In one embodiment, a physiological monitor measures light transmission through a patient's finger to determine arterial blood oxygen saturation. In some cases, however, the measured light signal contains noise, or other secondary signal, due to an event, such as patient movement during signal measurement. In such case, the signal measured by the physiological monitor includes a primary portion, related to the blood oxygen saturation of the patient, and a secondary portion, related to the noisy, erratic, motion-induced secondary signal. The physiological monitor processes the measured signal to determine the patient's blood oxygen saturation based upon the signal's primary portion.

[0030] In one embodiment, the physiological monitor utilizes a processor to determine a secondary reference signal n'(t) or N_{ref}. The secondary reference signal n'(t) is used to determine the primary portion of the measured signal. In one embodiment, the secondary reference signal n'(t) is input to a multi-variate process estimator, which removes the erratic, motion-induced secondary signal portions from the measured signal. In another embodiment, the processor determines a primary signal reference signal s'(t) which is used for display purposes or for input to a multi-variate process estimator to derive information about patient movement and venous blood oxygen saturation.

[0031] FIG. **1** illustrates an arterial blood oxygen saturation curve **100** representative of the sensitivity of blood oxygen saturation systems of the prior art. Such systems utilize two different wavelengths of light (such as red and infrared wavelength light) to determine blood oxygen saturation. The wavelengths used may be, for example, about 660 nm and about 905 nm. At 660 nm, deoxyhemoglobin has a higher absorption than oxyhemoglobin, while the reverse is the case at 905 nm. This difference in absorption between oxyhemoglobin and deoxyhemoglobin allows for the calculation of blood oxygen saturation levels.

[0032] In FIG. **1**, arterial blood oxygen saturation (SaO_2) is represented on the y-axis of the curve **100**. The x-axis represents ratios of a red wavelength light transmission signal and an infrared wavelength light transmission signal. An ideal saturation curve **102** would be highly accurate at all values. However, due to the limitations of using only two wavelengths of light, such systems typically operate between a lower range curve **104** and an upper range curve **106**. Such blood oxygen saturation systems typically exhibit highly accurate, low tolerance **107** measurements at high saturation values **108**, but at lower saturation values **110**, that accuracy decreases, and increased tolerance **111** results.

[0033] The arterial blood oxygen saturation curve **120** of a multi-wavelength physiological monitor in accordance with one embodiment of the present invention is shown in FIG. **2**. The multi-wavelength system utilizes at least three different wavelengths of light ($\lambda_1, \lambda_2, \ldots \lambda_n$) to determine blood oxygen saturation. Arterial blood oxygen saturation (S_aO_2) is represented on the y-axis of the curve **120**. The x-axis represents ratios of composite signals, each comprising signals based upon the light transmission of the various light wavelengths ($\lambda_1, \lambda_2, \ldots \lambda_n$). Each ratio r can be expressed by:

$$r = \frac{\sum_{i=1}^{n} \alpha_i NP_{RMS,i}}{\sum_{i=1}^{n} \beta_i NP_{RMS,i}}$$

where n is the number of wavelengths of light utilized by the multi-wavelength physiological monitor, $NP_{RMS,i}$ is the normalized plethysmographic waveform of the ith wavelength

light source, and α_i and β_i are vector coefficients of known constants that are determined based upon fitting and/or calibration using experimental data and/or model(s).

[0034] The curve **120** contains lower and upper limit range curves **122**, **124**. However, the lower and upper limit range curves **122**, **124** of the multi-wavelength physiological monitor are more linear than the lower and upper range curves **104**, **106** of the dual-wavelength blood oximeter described above, as illustrated in FIG. **1**. In addition, the lower and upper limit range curves **122**, **124** of the multi-wavelength physiological monitor exhibit higher accuracy and lower tolerance **126** than the dual-wavelength blood oximeter of FIG. **1**, particularly at lower arterial blood oxygen saturation levels. In certain cases, such as during the monitoring of neonates, or persons with low blood-oxygen saturation, it is desirable for the physiological monitor to exhibit increased accuracy at lower saturation levels. For example, when providing oxygen to a neonate, it is often critical that neither too much oxygen nor too little oxygen is provided. A multi-wavelength physiological monitor provides improved accuracy as well as an improved signal-to-noise ratio at lower perfusion levels.

[0035] A multi-wavelength physiological monitor provides additional advantages over a two-wavelength device, as well. For example, utilizing multiple wavelengths provide a multi-dimensional calibration curve, which can be used to provide multiple degrees of freedom to compensate for variation in other physiologically-related parameters. As discussed above, when only two wavelengths are used but there are more than two significant absorbers in the patient's tissue, the system may be underdetermined. Therefore, adding wavelengths sensitive to additional significant absorbers can help the system compensate for the additional significant absorbers and enable more accurate calculation of the concentration of each absorber and the blood oxygen saturation. For example, an eight wavelength physiological monitor utilizes an eight-dimensional calibration curve, which provides eight degrees of freedom to compensate for various physiologically-related parameters. Such parameters can include, for example, noise, motion, various hemodynamic parameters, and/or blood constituent concentrations and/or levels. On the other hand, the system may be overdetermined if, for example, more wavelengths are used than there are significant absorbers and/or wavelengths are used for constituents not present in the particular patient's blood.

[0036] Furthermore, traditional physiological monitors that utilize two light sources to derive a patient's plethysmographic signal generally require one light source's wavelength to fall in the red spectrum and the other light source's wavelength to fall in the infrared spectrum. However, a multi-wavelength physiological monitor advantageously provides the ability to utilize all infrared wavelength light sources and/or other non-red infrared light sources to derive an accurate plethysmographic waveform. One advantage of utilizing non-red wavelength light sources (for example, all infrared wavelength light sources) is that the multi-wavelength physiological monitor can be further configured to determine several blood constituent concentrations based upon signals measured from just the non-red light sources. For example, such a multi-wavelength physiological monitor can determine levels and/or concentrations of: methemoglobin (MetHb), carboxyhemoglobin (COHb), low hemoglobin levels, high hemoglobin levels, bilirubin, methylene blue, deoxyhemoglobin, and lipids.

[0037] The ability to measure a physiological parameter with a multi-dimensional system allows the system to compensate and account for the presence of other conditions that may affect the particular physiological parameter being measured. For example, many drugs cause the level of MetHb within a patient's blood to increase. MetHb also absorbs light at the two wavelengths used in a typical two-wavelength physiological monitor, which may cause inaccurate S_pO_2 readings. Increased levels of MetHb generally cause blood oxygen concentration level (e.g., S_pO_2) readings to decrease. A two-wavelength physiological monitor would provide reduced readings of blood oxygen concentration, but would not be able to identify the cause for the decreased reading, or to compensate for such readings. On the other hand, a multi-wavelength physiological monitor, such as any of the multi-wavelength physiological monitors described below, could not only identify the cause of decreased S_pO_2 readings, but also (or alternatively) compensate for such cause when calculating the patient's S_pO_2 level and/or signal. For example, to compensate for MetHb, one or more wavelengths sensitive to MetHb can be used. The wavelength(s) used can be, for example, about 760 nm and/or about 805 nm or the like. This allows for one or more additional equation (s) and degree(s) of freedom so that solving the system may account for the effect of the level of MetHb on blood oxygen saturation readings.

[0038] Similarly, the system can compensate for other blood constituents with the addition of wavelengths sensitive to the other blood constituents of interest. For example, carboxyhemoglobin absorbs about the same amount of 660 nm light as oxyhemoglobin. Therefore, a typical two-wavelength physiological monitor can mistake carboxyhemoglobin for oxyhemoglobin, which can result in normal blood oxygen saturation level readings even though the actual level is abnormal. For example, for every about 1% of carboxyhemoglobin circulating in the blood, the monitor may over read by about 1%. Selecting one or more additional wavelengths sensitive to carboxyhemoglobin, for example, about 610, 630, and/or 640 or the like, can allow the system to compensate for this effect. The system can compensate for other blood constituents, such as deoxyhemoglobin or lipids, with the addition of wavelengths sensitive to those constituents. More wavelengths can allow the system to compensate for more variables.

[0039] The various blood constituents mentioned above may not be orthogonal; rather they are often highly correlated with one another. Therefore, even using multiple wavelengths may not fully eliminate the effect of such constituents on the blood oxygen saturation level calculations, but it can reduce or minimize the effect and produce more accurate blood oxygen saturation level readings. In one embodiment, using eight wavelengths (including, for example, any of the wavelengths mentioned herein) can provide relatively more accurate readings of blood oxygen saturation levels relative to other numbers of wavelengths. However, the number of wavelengths that is most appropriate for a particular patient and that will provide the most accurate readings can vary based on such factors as the actual concentrations of blood constituents in the patient's blood, as well as the patient's condition, gender, age, or the like. In addition to improving the accuracy of blood oxygen saturation level readings, using multiple wavelengths can also provide relatively more accurate measurements of other parameters, including, for

example, the concentrations of any of the blood constituents or other parameters mentioned herein.

[0040] In one embodiment, the multi-wavelength physiological monitor compensates for conditions, such as motion and/or blood constituents that would cause a standard two-wavelength system to over- or under-react to the presence of such condition. Such compensation provides a more accurate, stable reading or a patient's physiological condition, including, but not limited to, their blood oxygen concentration and/or plethysmographic signal.

[0041] A schematic of one embodiment of a multi-wavelength physiological monitor for pulse oximetry is shown in FIGS. **3-5**. FIG. **3** depicts a general hardware block diagram of a multi-wavelength pulse oximeter **299**. A sensor **300** has n LEDs **302**, which in one embodiment are at least three light emitters. The n LEDs **302** emit light of different wavelengths ($\lambda_1, \lambda_2, \ldots \lambda_n$). In one embodiment, the n LEDs **302** include four, six, eight or sixteen LEDs of different wavelengths. In one embodiment, the n LEDs **302** are placed adjacent a finger **310**. A photodetector **320** receives light from the n LEDs **302** after it has been attenuated by passing through the finger. The photodetector **320** produces at least one electrical signal corresponding to the received, attenuated light. In one embodiment, the photodetector **320** is located opposite the n LEDs **302** on the opposite side of the finger **310**. The photodetector **320** is connected to front end analog signal conditioning circuitry **330**.

[0042] The front end analog signal conditioning circuitry **330** has outputs that are coupled to an analog to digital conversion circuit **332**. The analog to digital conversion circuit **332** has outputs that are coupled to a digital signal processing system **334**. The digital signal processing system **334** provides desired parameters as outputs for a display **336**. Outputs for the display **336** include, for example, blood oxygen saturation, heart rate, and a clean plethysmographic waveform.

[0043] The signal processing system also provides an emitter current control output **337** to a digital-to-analog converter circuit **338**. The digital-to-analog converter circuit **338** provides control information to emitter current drivers **340**. The emitter drivers **340** are coupled to the n light emitters **302**. The digital signal processing system **334** also provides a gain control output **342** for front end analog signal conditioning circuitry **330**.

[0044] FIG. **3**A illustrates one embodiment of the drivers **340** and the digital to analog conversion circuit **338**. As depicted in FIG. **3**A, the digital-to-analog conversion circuit **338** includes first and second input latches **321**, **322**, a synchronizing latch **323**, a voltage reference **324**, and a digital to analog conversion circuit **325**. The emitter current drivers **340** include first and second switch banks **326**, **327**, and n voltage to current converters **328**. LED emitters **302** of FIG. **3** are coupled to the output of the emitter current drives **340**.

[0045] The driver depicted in FIG. **3**A is advantageous in that the present inventors recognized that much of the noise in the oximeter **299** of FIG. **3** is caused by the LED emitters **302**. Therefore, the emitter driver circuit of FIG. **3**A is designed to minimize the noise from the emitters **302**. The first and second input latches **321**, **322** are connected directly to the DSP bus. Therefore, these latches significantly minimizes the bandwidth (resulting in noise) present on the DSP bus which passes through to the driver circuitry of FIG. **3**A. The output of the first and second input latches only changes when these latched detect their address on the DSP bus. The first input latch **321** receives the setting for the digital to analog converter circuit **325**. The second input latch **322** receives switching control data for the switch banks **326**, **327**. The synchronizing latch **323** accepts the synchronizing pulses which maintain synchronization between the activation of emitters **302** and the analog to digital conversion circuit **332**.

[0046] The voltage reference is chosen as a low noise DC voltage reference for the digital to analog conversion circuit **325**. In addition, in the present embodiment, the voltage reference has a lowpass output filter with a very low corner frequency (e.g., 1 Hz in the present embodiment). The digital to analog converter **325** also has a lowpass filter at its output with a very low corner frequency (e.g., 1 Hz). The digital to analog converter provides signals used to drive each of the emitters **302**.

[0047] In the present embodiment, the output of the voltage to current converters **328** are switched such that, only one emitter is active at any given time. In addition, the voltage to current converter for the inactive emitter is switched off at its input as well, such that it is deactivated. This reduces noise from the switching and voltage to current conversion circuitry. In the present embodiment, low noise voltage to current converters **328** are selected (e.g., Op 27 Op Amps), and the feedback loop is configured to have a low pass filter to reduce noise. In the present embodiment, the low pass filtering function of the voltage to current converters **328** has a corner frequency of just above 625 Hz, which is the switching speed for the emitters **302**, as further discussed below. Accordingly, the driver circuit embodiment of FIG. **3**A, minimizes the noise of the emitters **302**.

[0048] In general, the n light emitters **302** each emit light energy of a different wavelength, which is absorbed by the finger **310** and received by the photodetector **320**. The photodetector **320** produces an electrical signal which corresponds to the intensity of the light energy striking the photodetector **320**. The front end analog signal conditioning circuitry **330** receives the intensity signals and filters and conditions these signals as further described below for further processing. The resultant signals are provided to the analog-to-digital conversion circuitry **332**, which converts the analog signals to digital signals for further processing by the digital signal processing system **334**. The digital signal processing system **334** utilizes the signals in order to provide what will be called herein a "saturation transform." It should be understood, that for parameters other than blood saturation monitoring, the saturation transform could be referred to as a concentration transform, in-vivo transform, or the like, depending on the desired parameter. The term "saturation transform" is used to describe an operation which converts the sample data from time domain to saturation domain values, as will be apparent from the discussion below. In the present embodiment, the output of the digital signal processing system **334** provides clean plethysmographic waveforms of the detected signals and provides values for oxygen saturation and pulse rate to the display **336**.

[0049] It should be understood that in different embodiments of the present invention, one or more of the outputs may be provided. The digital signal processing system **334** also provides control for driving the n light emitters **302** with an emitter current control signal on the emitter current control output **337**. This value is a digital value which is converted by the digital-to-analog conversion circuit **338**, which provides a control signal to the emitter current drivers **340**. The emitter current drivers **340** provide the appropriate current drive for

the n light emitters **302**. Further detail of the operation of the multi-wavelength physiological monitor for pulse oximetry is explained below.

[0050] In the present embodiment, the n light emitters **302** are driven via the emitter current driver **340** to provide light transmission with digital modulation at 625 Hz. In the present embodiment, the n light emitters **302** are driven at a power level that provides an acceptable intensity for detection by the detector **320** and for conditioning by the front end analog signal conditioning circuitry **330**. Once this energy level is determined for a given patient by the digital signal processing system **334**, the current level for the n light emitters **302** is maintained substantially constant. It should be understood, however, that the current could be adjusted for changes in the ambient room light and other changes that would affect the voltage input to the front end analog signal conditioning circuitry **330**.

[0051] In one embodiment, the n light emitters **302** are modulated as follows: for one complete 625 Hz cycle, each emitter **302** is activated for one ½n cycle, and off for the remaining (2n−1)/2n cycle. In order to only receive one signal at a time **302**, the emitters are cycled on and off alternatively, in sequence, with each only active for a ½n cycle per 625 Hz cycle, with a ½n cycle separating the active times. The light signal is attenuated (e.g., amplitude modulated) by the pumping of blood through the finger **310** (or other sample medium). The attenuated (e.g., amplitude modulated) signal is detected by the photodetector **320** at the 625 Hz carrier frequency for the multi-wavelength light. Because only a single photodetector **320** is used, the photodetector **320** receives all light wavelength signals to form a composite time division signal.

[0052] The composite time division signal is provided to the front analog signal conditioning circuitry **330**. Additional detail regarding the front end analog signal conditioning circuitry **330** and the analog to digital converter circuit **332** is illustrated in FIG. **4**. As depicted in FIG. **4**, in one embodiment, the front end circuitry **330** has a preamplifier **342**, a high pass filter **344**, an amplifier **346**, a programmable gain amplifier **348**, and a low pass filter **350**. In one embodiment, the preamplifier **342** is a transimpedance amplifier that converts the composite current signal from the photodetector **320** to a corresponding voltage signal, and amplifies the signal. In the present embodiment, the preamplifier has a predetermined gain to boost the signal amplitude for ease of processing. In the present embodiment, the source voltages for the preamplifier **342** are −15 VDC and +15 VDC. As will be understood, the attenuated signal contains a component representing ambient light as well as a component representing the each of the multi-wavelengths of light over time. If there is light in the vicinity of the sensor **300** other than the multi-wavelengths of light from the n light emitters **302**, this ambient light is detected by the photodetector **320**. Accordingly, the gain of the preamplifier is selected in order to prevent the ambient light in the signal from saturating the preamplifier under normal and reasonable operating conditions.

[0053] In one embodiment, the preamplifier **342** includes an Analog Devices AD743JR OpAmp. This transimpedance amplifier is particularly advantageous in that it exhibits several desired features for the system described, such as: low equivalent input voltage noise, low equivalent input current noise, low input bias current, high gain bandwidth product, low total harmonic distortion, high common mode rejection, high open loop gain, and a high power supply rejection ratio.

[0054] The output of the preamplifier **342** is coupled to an input of the high pass filter **344**. The output of the preamplifier also provides a first input **346** to the analog to digital conversion circuit **332**. In the present embodiment, the high pass filter is a single-pole filter with a corner frequency of about ½-1 Hz. However, the corner frequency is readily raised to about 90 Hz in one embodiment. As will be understood, the 625 Hz carrier frequency of the multi-wavelength light signal is well above a 90 Hz corner frequency. The high-pass filter **344** has an output coupled as an input to an amplifier **346**. In the present embodiment, the amplifier **346** comprises a unity gain amplifier. However, the gain of the amplifier **346** is adjustable by the variation of a single resistor. The gain of the amplifier **346** is increased if the gain of the preamplifier **342** is decreased to compensate for the effects of ambient light.

[0055] The output of the amplifier **346** provides an input to a programmable gain amplifier **348**. The programmable gain amplifier **348** also accepts a programming input from the digital signal processing system **334** on a gain control signal line **343**. In one embodiment, the gain of the programmable gain amplifier **348** is digitally programmable. The gain is adjusted dynamically at initialization or at sensor placement due to changes in the medium (e.g., the finger) and due to variations in the medium from patient to patient. Therefore, a dynamically adjustable amplifier is provided by the programmable gain amplifier **348** in order to obtain a signal suitable for processing.

[0056] The programmable gain amplifier **348** is also advantageous in an alternative embodiment in which the emitter drive current is held constant. In the present embodiment, the emitter drive current is adjusted for each patient in order to obtain the proper dynamic range at the input of the analog to digital conversion circuit **332**. However, changing the emitter drive current can alter the emitter wavelength, which in turn affects the end result in oximetry calculations. Accordingly, in another embodiment, it is advantageous to fix the emitter drive current for all patients. In an alternative embodiment of the present invention, the programmable gain amplifier can be adjusted by the DSP in order to obtain a signal at the input to the analog to digital conversion circuit which is properly within the dynamic range (+3 V to −3 V in the present embodiment) of the analog to digital conversion circuit **332**. In this manner, the emitter drive current could be fixed for all patients, eliminating wavelength shift due to emitter current drive changes.

[0057] The output of the programmable gain amplifier **348** couples as an input to a low-pass filter **350**. Advantageously, the low pass filter **350** is a single-pole filter with a corner frequency of approximately 10 kHz in the present embodiment. This low pass filter provides anti-aliasing in the present embodiment.

[0058] The output of the low-pass filter **350** provides a second input **352** to the analog-to-digital conversion circuit **332**. In the present embodiment, the analog-to-digital conversion circuit **332** comprises a first analog-to-digital converter **354** and a second analog-to-digital converter **356**. Advantageously, the first analog-to-digital converter **354** accepts input from the first input **346** to the analog-to-digital conversion circuit **332**, and the second analog to digital converter **356** accepts input on the second input **352** to the analog-to-digital conversion circuitry **332**.

[0059] In one embodiment, the first analog-to-digital converter **354** is a diagnostic analog-to-digital converter. The diagnostic task (performed by the digital signal processing

system) is to read the output of the detector as amplified by the preamplifier **342** in order to determine if the signal is saturating the input to the high-pass filter **344**. In the present embodiment, if the input to the high pass filter **344** becomes saturated, the front end analog signal conditioning circuits **330** provides a "0" output. Alternatively, in another embodiment, a first analog-to-digital converter **354** is not used.

[0060] The second analog-to-digital converter **356** accepts the conditioned composite analog signal from the front end signal conditioning circuitry **330** and converts the signal to digital form. In the present embodiment, the second analog to digital converter **356** comprises a single-channel, delta-sigma converter. In the present embodiment, a Crystal Semiconductor CS5317-KS delta-sigma analog to digital converter is used. Such a converter is advantageous in that it is low cost and exhibits low noise characteristics. More specifically, a delta-sigma converter consists of two major portions: a noise modulator and a decimation filter. The selected converter uses a second order analog delta-sigma modulator to provide noise shaping. Noise shaping refers to changing the noise spectrum from a flat response to a response where noise at the lower frequencies has been reduced by increasing noise at higher frequencies. The decimation filter then cuts out the reshaped, higher frequency noise to provide 16-bit performance at a lower frequency. The present converter samples the data 128 times for every 16 bit data word that it produces. In this manner, the converter provides excellent noise rejection, dynamic range and low harmonic distortion, which help in critical measurement situations like low perfusion and electrocautery.

[0061] In addition, by using a single-channel converter, there is no need to tune two or more channels to each other. The delta-sigma converter is also advantageous in that it exhibits noise shaping, for improved noise control. An exemplary analog to digital converter is a Crystal Semiconductor CS5317. In the present embodiment, the second analog to digital converter **356** samples the signal at a 20 kHz sample rate. The output of the second analog to digital converter **356** provides data samples at 20 kHz to the digital signal processing system **334** (FIG. **3**).

[0062] The digital signal processing system **334** is illustrated in additional detail in FIG. **5**. In the present embodiment, the digital signal processing system includes a microcontroller **360**, a digital signal processor (DSP) **362**, a program memory **364**, a sample buffer **366**, a data memory **368**, a read only memory **370** and communication registers **372**. In one embodiment, the digital signal processor **362** is an Analog Devices AD 21020, although other digital signal processors may be employed, as is well known by those of skill in the art. In one embodiment, the microcontroller **360** comprises a Motorola 68HC05, with built in program memory. In the present embodiment, the sample buffer **366** is a buffer which accepts the 20 kHz sample data from the analog to digital conversion circuit **332** for storage in the data memory **368**. In the present embodiment, the data memory **368** comprises 32 kWords (words being 40 bits in the present embodiment) of static random access memory. Other chips, data rates and data memory configurations may be employed, as is well known to those of skill in the art.

[0063] In one embodiment, the microcontroller **360** is coupled to the DSP **362** via a conventional JTAG Tap line. The microcontroller **360** transmits the boot loader for the DSP **362** to the program memory **364** via the Tap line, and then allows the DSP **362** to boot from the program memory **364**. The boot loader in program memory **364** then causes the transfer of the operating instructions for the DSP **362** from the read only memory **370** to the program memory **364**. Advantageously, the program memory **364** is a very high speed memory for the DSP **362**. The microcontroller **360** provides the emitter current control and gain control signals via the communications register **372**.

[0064] FIGS. **6-10** depict functional block diagrams of the operations of the multi-wavelength pulse oximeter **299** that in one embodiment are executed by the digital signal processing system **334**. The signal processing functions described below are carried out by the DSP **362** in the present embodiment, with the microcontroller **360** providing system management. In the present embodiment, the operation is software/firmware controlled. FIG. **6** depicts a generalized functional block diagram for the operations performed on the 20 kHz sample data entering the digital signal processing system **334**. As illustrated in FIG. **6**, a demodulation operation, as represented in a demodulation module **400**, is first performed. Sub-sampling, as represented by sub-sampling operation **402**, is then performed on the resulting data. Certain statistics are calculated, as represented in a statistics module **404**. A saturation transform is performed, as represented in a saturation transform module **406**, on the data resulting from the sub-sampling operation **402**. The data subjected to the statistics operations and the data subjected to the saturation transform operations are forwarded to saturation operations, as represented by a saturation calculation module **408** and pulse rate operations, as represented by pulse rate calculation module **410**.

[0065] In general, the demodulation operation separates each of the multi-wavelength signals from the composite signal and removes the carrier frequency, leaving raw data points. The raw data points are provided at intervals (e.g., at 625 Hz) to the sub-sampling operation **402**, which in one embodiment, reduces the samples by an order of 10 from samples at 625 Hz to samples at 62.5 Hz. The sub-sampling operation also provides some filtering on the samples. The resulting data is subjected to statistics and saturation transform operations **404**, **406** to calculate a saturation value, which is very tolerant to motion artifacts and other noise in the signal. The saturation value is ascertained in the saturation calculation module **408**, and a pulse rate and a clean plethysmographic waveform are obtained through the pulse rate module **410**. Additional details regarding the various operations are provided in connection with FIGS. **7-10**.

[0066] FIG. **7** illustrates one embodiment of the operation of the demodulation module **400**. One embodiment of a composite, modulated signal format is depicted in FIG. **7**. One full 625 Hz cycle of the n-wavelength, composite signal is depicted in FIG. **7** with the first ½n cycle including the first light wavelength signal plus ambient light signal, the second ½n cycle including an ambient light signal, the third ½n cycle including the second light wavelength signal plus ambient light signal, and the fourth ½n cycle including an ambient light signal. In one embodiment, this pattern repeats n times, wherein the $(2n-1)^{th}$ ½ n cycle includes the nth light wavelength signal plus an ambient light signal, and the $2n^{th}$ cycle includes an ambient light signal.

[0067] Alternatively, in another embodiment, the first cycle of the composite signal includes the first light wavelength signal plus an ambient light signal, and the second cycle of the composite signal includes the second light wavelength signal plus an ambient light signal. This pattern repeats to the nth cycle of the composite signal, which includes the nth wave-

length signal plus an ambient light signal. In such embodiment, the $(n+1)^{th}$ cycle includes only an ambient light signal.

[0068] As depicted in FIG. **7**, when a 20 kHz sampling frequency is utilized, the single full cycle at 625 Hz described above comprises 32 samples of 20 kHz data, eight samples relating to the first wavelength of light plus ambient light, eight samples relating to ambient light, eight samples relating to the second wavelength of light plus ambient light, finally eight samples related to ambient light, etc. This pattern repeats for each of the n wavelength of light.

[0069] Because the signal processing system **334** controls the activation of the light emitters **302**, the entire system is synchronous. In one embodiment, the data is synchronously divided (and thereby demodulated) into 2n 8-sample packets, with a time division demultiplexing operation as represented in a demultiplexing module **421**. One eight-sample packet **422** represents the first wavelength of light plus ambient light signal, a second eight-sample packet **424** represents an ambient light signal, a third eight-sample packet (not shown) represents the attenuated second wavelength of light plus ambient light signal, a fourth eight-sample packet (not shown) represents the ambient light signal. This structure repeats until the $(2n-1)^{th}$ eight-sample packet **426**, which represents the attenuated n^{th} wavelength of light plus ambient light signal, and $2n^{th}$ eight-sample packet **428**, which represents an ambient light signal. A select signal synchronously controls the demultiplexing operation so as to divide the time-division multiplexed composite signal at the input of the demultiplexer **421** into its n subparts.

[0070] In one embodiment, the last several samples from each packet are then processed as follows. A sum of the last four samples from each packet is calculated, as represented in the summing operations **430** of FIG. **7**. In the present embodiment, the last four samples are used because a low pass filter in the analog to digital converter **356** of the present embodiment has a settling time. However, any number of samples may be so summed. The selection of the number of samples to be summed will be determined based at least in part on the settling time of the n LEDs **302** (not shown). Collecting the last four samples from each 8-sample packet allows the previous signal to clear. This summing operation provides an integration operation which enhances noise immunity. The sum of the respective ambient light samples is then subtracted from the sum of each of the individual wavelength samples, as represented in the subtraction modules **438**. It should be understood that in one embodiment, for n wavelengths of light, there will be n subtraction modules **438**. The subtraction operation provides some attenuation of the ambient light signal present in the data. In the present embodiment, it has been found that approximately 20 dB attenuation of the ambient light is provided by the operations of the subtraction modules **438**. The resultant individual wavelength sum values are divided by the number of samples summed in summing operations **430**. In the present embodiment, the sum values are divided by four, as represented in the divide modules **442**. Each resultant value provides one sample each of each of the individual wavelengths light signals at 625 Hz.

[0071] It should be understood that the carrier frequency has been removed by the demodulation operation **400**. In one embodiment, the 625 Hz sample data at the output of the demodulation operation **400** is sample data without the carrier frequency. In order to satisfy Nyquist sampling requirements, less than 20 Hz is used (understanding that the human pulse is about 25 to 250 beats per minute, or about 0.4 Hz-4 Hz). Accordingly, the 625 Hz resolution is reduced to 62.5 Hz in the sub-sampling operation **402** (not shown). Although in the present embodiment the sub-sampling operation **400** effectively reduces the data rate by 10:1, other such sub-sampling ratios may be used. The term "sub-sampling," in addition to its ordinary meaning, is intended to include decimation and sub-sampling at any appropriate rate or ratio. Such methods are well known to those of skill in the art.

[0072] FIG. **8** illustrates the operations of one embodiment of the sub-sampling module **402** of FIG. **6**. The multi-wavelength light sample data is provided at 625 Hz to corresponding buffers or filters **450**. It should be understood that in one embodiment, for n wavelengths of light, there are n corresponding buffers or filters **450**. In the present embodiment, the multi-wavelength light buffers/filters **450** are 519 samples deep, although other such buffers or filters may be used, as is well known to those of skill in the art. In one embodiment, the buffer filters **450** function as continuous first-in, first-out buffers (FIFO buffers). The 519 samples of each buffer filter **450** are subjected to low-pass filtering. Preferably, the low-pass filtering has a cutoff frequency of approximately 7.5 Hz with attenuation of approximately −110 dB. The buffer/filters **450** form a Finite Impulse Response (FIR) filter with coefficients for 519 taps. In order to reduce the sample frequency by ten, the low-pass filter calculation is performed every ten samples, as represented in sub-sample modules **454**. In other words, with the transfer of each new ten samples into the buffer/filters **450** a new low pass filter calculation is performed by multiplying the impulse response (coefficients) by the 519 filter taps. Each filter calculation provides one output sample for respective output buffers **458**. In the present embodiment, the output buffers **458** are also continuous FIFO buffers that hold 570 samples of data. The 570 samples provide respective samples or packets (also denoted "snapshot" herein) of samples. The output buffers **458** provide sample data to the statistics operation module **404**, saturation transform module **406**, and the pulse rate module **410**, as illustrated in FIG. **6**.

[0073] FIG. **9** illustrates additional functional operation details of the statistics module **404**. In summary, the statistics module **404** provides first order oximetry calculations and RMS signal values for each of the n wavelengths of light. The statistics module **404** also provides a cross-correlation output which indicates a cross-correlation between the n wavelengths of light.

[0074] As represented in FIG. **9**, the statistics module **404** receives n packets of samples from the output buffers **458** (not shown) of the sub-sampling module **402** of FIGS. **6** and **8**. In one embodiment, the samples include 570 samples at 62.5 Hz which represent the attenuated n wavelengths of light signals with the carrier frequency removed. Each packet is normalized with a log function, as represented in the n log modules **480**.

[0075] The signals are then subjected to bandpass filtering, as represented in the n bandpass filter modules **488**. In the present embodiment, with 570 samples in each packet, the bandpass filters are configured with 301 taps to provide a FIR filter with a linear phase response and little or no distortion. In the present embodiment, the bandpass filter has a pass band from 34 beats/minute to 250 beats/minute. The 301 taps slide over each 570 sample packet in order to obtain 270 filtered samples for each of the n filtered wavelength signal. In one embodiment, the n bandpass filters **488** remove the DC in the

signal. However, in another embodiment, addition DC removal operations (not shown) may be provided to assist in DC removal.

[0076] After filtering, the last j samples from each packet (each packet now containing 270 samples in the present embodiment) are selected for further processing, as represented in the n select last j samples modules **492**. In one embodiment, j equals 120, and the last 120 samples are selected in the select last j samples modules **492**. In one embodiment, 120 samples are selected because the first 150 samples fall within the settling time for the saturation transfer module **406**. The saturation transfer module **406** processes the same data packets, as further discussed below.

[0077] In the present embodiment, saturation equation calculations are performed on each 120-sample packet. In the present embodiment, the saturation calculations are performed in two different ways. For one calculation, the 120-sample packets are processed to obtain each packet's overall RMS value, as represented in the λ_1 through λ_n RMS modules **496**. It should be understood that in the present embodiment there are n such RMS modules, although as few as one RMS module may be used. The resultant RMS values for each of the n wavelengths of light provide input values to a first ratio operation **500**, which provides its output as an input to a saturation equation module **502**. The ratio operation **500** calculates a ratio of the various signals based upon the multi-wavelength model described above, and illustrated as:

$$r = \frac{\sum_{i=1}^{n} \alpha_i NP_{RMS,i}}{\sum_{i=1}^{n} \beta_i NP_{RMS,i}}$$

[0078] The ratio of the intensity of different light wavelengths may be used to determine the oxygen saturation of the patient. In one embodiment, the ratio is provided to a saturation equation module **502**, which includes a look-up table, a polynomial, or the like. The saturation equation module **502** provides a saturation values at its output **504** based upon the ratio. In another embodiment, the n wavelengths' individual RMS values are also provided as outputs of the statistics operations module **404**.

[0079] The n 120-sample packets (corresponding to each of the n wavelengths of light) are subjected to a cross-correlation operation as represented in a first cross-correlation module **506**. The first cross-correlation module **506** determines if good correlation exists between the various light wavelength signals. This cross correlation is advantageous for detecting defective or otherwise malfunctioning detectors. The cross correlation is also advantageous in detecting when the signal model is satisfied. The signal model of the multi-wavelength physiological monitor is described in greater detail above with respect to FIG. **2**, and in greater detail below, with respect to FIG. **10**. If correlation becomes too low between the signals, the signal model is not satisfied. In order to determine whether the signal model is satisfied, the normalized cross correlation can be computed by the cross-correlation module **506** for each snapshot of data.

[0080] In one embodiment, correlation between any two wavelength signals x_1 and x_2 is determined according to:

$$\frac{\sum_j x_{1,j} x_{2,j}}{\sqrt{\sum_j x_{1,j}}\sqrt{\sum_j x_{2,j}}}$$

For n wavelengths, a cross-correlation matrix, Corr $[x\,x^T]$, is determined, where $x \epsilon R^n$. In one embodiment, a minimum value of the cross-correlation matrix is determined. The minimum value may be determined by looking for the minimum value within the matrix, or the minimum eigenvalue of the matrix. Other methods may be used, as are well known to those of skill in the art.

[0081] If the cross-correlation minimum value is too low, the oximeter **299** provides a warning (e.g., audible, visual, etc.) to the operator. In the present embodiment, if a selected snapshot yields a normalized correlation of less than 0.75, the snapshot does not qualify. Signals which satisfy the signal model will have a correlation greater than the threshold.

[0082] In one embodiment, the 120-sample packets are also subjected to a second saturation operation and cross correlation in the same manner as described above, except the 120-sample packets are first divided into equal bins of samples (e.g., five bins of 24 samples each). The RMS, ratio, saturation, and cross correlation operations are performed on a bin-by-bin basis. These operations are represented in the divide into equal bins modules **510** the second RMS modules **514** the second ratio module **518**, the second saturation equation module **520**, and the second cross-correlation module **522**, as illustrated in FIG. **9**. In one embodiment, the divide into equal bins modules **510** divides the data into five equal bins. However, the divide into equal bins modules **510** may divide the data into any desirable number of equal bins, for example, 7 bins, 10 bins or 20 bins.

[0083] FIG. **10** illustrates additional detail regarding the saturation transform module **406** of FIG. **6**. As illustrated in FIG. **10**, the saturation transform module **406** includes log module **537**, bandpass filter module **538**, signal selector module **536**, reference generator **530**, a multi-variate process estimator **531**, a master power curve module **554**, a divide into equal bins module **556**, and a bin power curve module **533**. In another embodiment, the saturation transform module has a reference processor, a correlation canceller, and an integrator to provide a power curve for separate signal coefficients. Reference processors, correlation cancellers, and integrators are well known to those of skill in the art, and are described in U.S. Pat. Nos. 5,632,272 and 5,490,505, both of which are incorporated by reference herein in their entireties.

[0084] As depicted in FIG. **10**, the saturation transform module **406** receives the n packets (one packet for each wavelength of light) from the sub-sampling module **402** (not shown) of FIG. **6**. In one embodiment, each of the n packets contains 570 samples, although other sized packets may be employed. The data stored in the n packets, indicated in FIG. **10** as λ_1 Signal Data, λ_2 Signal Data, . . . λ_n Signal Data, is processed by log module **537**. Log module **537** performs a logarithmic function on each of the n packets, similar to the log module **480** of the statistics module **404** described above with reference to FIG. **9**. The output of the log module **537** is input to a bandpass filter module **538**. In one embodiment, the bandpass filter module **538** performs the same type of filtering as the n bandpass filters **488** of the statistics module **404**

described above with reference to FIG. **9**. Accordingly, each set of 570 samples subjected to bandpass filtering results in 270 remaining samples. The resulting data at the n outputs **542** of the bandpass filter module **538** are, in one embodiment, n vectors of 270 samples. Each output **542** represents the normalized plethysmographic waveform of the corresponding wavelength of light. The outputs **542** are provided to a signal selector module **536** and a reference generator **530**.

[0085] A plurality of possible saturation values (the "saturation axis scan," or SaO_{2_scan} values) are provided to the saturation reference processor **530** in addition to the normalized plethysmographic waveform outputs **542**. In the present embodiment, 117 saturation values are provided as the saturation axis scan. In a preferred embodiment, the 117 saturation values range uniformly from a blood oxygen saturation of 34.8 to 105.0. Accordingly, in the present embodiment, the 117 saturation values provide an axis scan for the reference generator **530**, which generates a reference signal N_{ref} for use by the multi-variate process estimator **531**.

[0086] In the present embodiment, the multi-variate process estimator **531** includes a pseudo-inverse, as is known to those of skill in the art. In another embodiment, the multi-variate process estimator **531** is formed by a joint process estimator and a low pass filter. Details of a suitable joint process estimator are provided in U.S. Pat. No. 5,632,272, incorporated by reference herein. However, it will be understood by those of skill in the art that a variety of such processing structures may be utilized. For example, in another embodiment, a correlation canceller, an adaptive linear combiner, an adaptive noise filter (e.g., as shown in FIG. **10**A), an adaptive noise canceller, an adaptive linear lattice, a neural network, a radial basis, or a voltera are used individually or in combination, instead of or in addition to the pseudo-inverse embodiment of the multi-variate process estimator **531**. Such processing structures are well known to those of skill in the art, and require no further explanation herein.

[0087] It should be understood that the scan values could be chosen to provide higher or lower resolution than 117 scan values. In one embodiment, the scan values are non-uniformly spaced.

[0088] As illustrated in FIG. **10**, the reference processor **530** accepts the saturation axis scan values as an input and provides a reference signal N_{ref} as an output. However, in another embodiment, saturation axis scan values are provided to a saturation equation module (not shown). In such embodiment, the saturation equation module provides outputs "r_n" that correspond to the plurality of scan value discussed above. The saturation equation simply provides a known ratio that corresponds to the saturation value received as an input based upon data contained within a look-up table, or based upon a known polynomial relationship between the saturation axis scan values and the output "r_n".

[0089] When a saturation equation module is employed, the ratio "r_n" is provided by the saturation equation module as an input to the reference generator **530**, along with the sample packets for each of the n light wavelengths. When a saturation equation module is not employed, as illustrated in FIG. **10**, a plurality of "r_n" values are provided as the saturation axis. In one embodiment, the "r_n" values are represented as $\rho(SaO_{2_scan})$, a row vector of known constants. The reference generator **530** processes the inputs as follows.

[0090] The reference generator **530** output N_{ref} is a vector which equals $\rho(SaO_{2_scan})x$, where x is a vector of the normalized plethysmographic waveforms for each of the n wavelengths of light signals x_i (such as outputs **542**) and $\rho(SaO_{2_scan})$ is a row vector of known constants.

$$\rho(SaO_{2_scan})=f^{-1}(SaO_{2_scan})b^T-a^T, \rho\epsilon R^{1xn}.$$

[0091] This noise reference signal can be derived from the following conditions and relationships. For example, in one embodiment, arterial blood oxygen saturation (SaO_2) is estimated with the following generalized ratiometric model:

$$SaO2 = f\left(\frac{a^T x_{a,rms}}{b^T x_{a,rms}} + \text{bias}\right), \text{ with } a,\ b,\ x_{a,rms} \in R^n \text{ and bias} \in R. \tag{1}$$

[0092] Within the ratiometric model: (i) a, b and bias are known constants derived from and/or defined based on fitting and/or calibration using experimental data and/or one or more models; (ii) $x_{a,rms}$ is a vector of arterial rms-normalized plethysmographic data. For example, in the case of a nine-wavelength system, n=9, and each entry of x_a is arterial rms-normalized plethysmographic data associated to a specific wavelength; and (iii) f:R→R is a functional mapping defining a "calibration" curve. It may assume any shape as long as it is invertible.

[0093] In one embodiment, the venous component of the plethysmographic signal, n_v, is linearly added to the arterial plethysmographic signal such that:

$$x=x_a+n_v, x, x_a, n_v \epsilon R^n. \tag{2}$$

[0094] In the foregoing equation (2), x represents the instantaneous bulk normalized plethysmographic signal, composed of arterial, x_a, and venous, n_v, portions. The venous portion is assumed to be and/or corresponds to the noise component of the bulk normalized plethysmographic signal.

[0095] In one embodiment, all the entries of n_v have the same frequency content. For example, if $n_v=[n_1\ n_2\ n_3]^T$, then $corr(n_1,n_2)=corr(n_1,n_3)=corr(n_2,\ n_3)=1$, which implies that motion affects evenly all the wavelengths, since it is caused by a single noise source (e.g., the change in venous blood volume). Furthermore, x_a and n_v are assumed to be uncorrelated.

[0096] In one embodiment, a venous noise reference signal is derived from the parameters and relationships provided above. For example, replacing in equation (1), the rms version, $x_{a,rms}$, with its instantaneous counterpart, x_a, it follows that,

$$((f^{-1}(SaO2)-\text{bias})b^T-a^T)x_a=0.$$

[0097] Replacing x_a with (2) yields:

$$((f^{-1}(SaO2)-\text{bias})b^T-a^T)n_v=((f^{-1}(SaO2)-\text{bias})b^T-a^T)\ x. \tag{3}$$

[0098] It follows from equation (3) that all entries of vector n_v can be linearly related to a single source (for example, the change in venous blood due to motion, v_v) as follows:

$$n_v=\alpha v_v,\ \alpha\epsilon R^n, \text{ and } v_v\epsilon R. \tag{4}$$

[0099] In one embodiment, the vector of parameters, α, is not a function of motion artifacts, but is instead a function of the physiological parameters of the site being used for measurement. Therefore, it has much slower variations when compared to the source of motion, v_v, and as a result, it can be assumed constant during a few arterial-plethysmographic cycles.

[0100] Replacing (4) in (3) yields:

$$((f^{-1}(\mathrm{SaO2})-\mathrm{bias})b^T-a^T)\alpha v_v=((f^{-1}(\mathrm{SaO2})-\mathrm{bias})b^T-a^T)x. \quad (5)$$

[0101] During the time interval of a few plethysmographic cycles, if SaO2 is assumed to be a constant, it follows from (5) that:

$$\beta(\mathrm{SaO2})v_v=\rho(\mathrm{SaO2})x, \quad (6)$$

where, β is a unknown scalar, is only a function of the saturation value, such that:

$$\beta(\mathrm{SaO2})=((f^{-1}(\mathrm{SaO2})-\mathrm{bias})b_T-a^T)\alpha,\beta\epsilon R,$$

and ρ is a row vector of known constants, is also only a function of the saturation value, such that:

$$\rho(\mathrm{SaO2})=((f^{-1}(\mathrm{SaO2})-\mathrm{bias})b^T-a^T),\rho\epsilon R^{lxn}.$$

[0102] Equation (6) implies that if the correct value for SaO2 is applied to it, the venous noise signal will be a linear combination of the bulk plethysmographic signals, entries of vector x.

[0103] Therefore, in equation (6), $\beta(\mathrm{SaO2})v_v$ is the noise reference signal that can be used in combination with an adaptive linear noise canceller to remove the venous noise signal from the bulk plethysmographic signal.

[0104] As a result, the venous-noise-reference-signal equation can be written as:

$$N_{ref}=\rho(\mathrm{SaO2})x \quad (7)$$

[0105] The vector x is provided as the outputs **542** illustrated in FIG. **10**. The SaO_{2_scan} values are the "r_n" values provided as the saturation axis, and a and b are known constants defined based on fitting and/or calibration using experimental data and/or models. This operation is completed for each of the saturation scan values (e.g., 117 possible values in the present embodiment). Accordingly, the resultant data can be described as 117 reference signal vectors of 570 data points each, hereinafter referred to as the reference signal vectors. This data can be stored in an array or any such data structure as is well known to those of skill in the art.

[0106] In the present embodiment, as described above, the outputs **542** are also provided to a signal selector module **536**. One of the output signals **542** is selected by the signal selector module **536** for further processing by the multi-variate process estimator **531**. The selected signal is referred to as X_{sel}. It is understood by those of skill in the art that any one of the output signals **542** may be selected by the signal selector module **536** for further processing.

[0107] In one embodiment, the multi-variate process estimator **531** includes a pseudo-inverse, which is used to determine a weight vector w associated with the reference signal N_{ref} and the selected signal. In one embodiment, the multi-variate process estimator **531** creates multiple single-column vectors of time-shifted data from the reference signal N_{ref}. For example, in one embodiment, the multi-variate process estimator **531** creates single-column vectors A, where:

$$A=\begin{bmatrix}\begin{bmatrix}N_{ref_1}\\N_{ref_2}\\N_{ref_3}\\N_{ref_4}\\\vdots\end{bmatrix}\begin{bmatrix}N_{ref_7}\\N_{ref_8}\\N_{ref_9}\\N_{ref_10}\\\vdots\end{bmatrix}\begin{bmatrix}N_{ref_13}\\N_{ref_14}\\N_{ref_15}\\N_{ref_16}\\\vdots\end{bmatrix}\cdots\end{bmatrix}$$

In such embodiment, a pseudo-inverse is determined as $(A^TA)^{-1}A^T$. The weight vector w may then be determined by multiplying the pseudo-inverse by the selected signal (X_{sel}) from the signal select module **536**. The resulting vector w may be expressed as: $w=(A^TA)^{-1}A^Tx_{sel}$. The output vectors w of the multi-variate process estimator **531** are provided to a master power curve module **554** and a divide into equal bins module **556**.

[0108] The divide into equal bins module **556** divides each of the output vectors into bins having equal numbers of data points. In one embodiment, the divide into equal bins module **556** divides each of the output vectors into five bins, each containing the same number of data points (e.g., with 120 data points per vector, each bin could have 24 data points). Each bin is then provided to a bin power curves module **558**.

[0109] In one embodiment, the master power curve module **554** performs a saturation transform as follows. For each output vector, the sum of the squares of the data points is determined. This provides a sum of squares value corresponding to each output vector (each output vector corresponding to one of the saturation scan values). These values provide the basis for a master power curve **555**, as further represented in FIG. **11**. The horizontal axis of the power curve represents the saturation axis scan values and the vertical axis represents the sum of squares value (or output energy) for each output vector. In one embodiment, as depicted in FIG. **11**, each of the sum of squares is plotted with the magnitude of the sum of squares value plotted on the vertical "energy output" axis at the point on the horizontal axis of the corresponding saturation scan value which generated that output vector. This results in a master power curve **558**, an example of which is depicted in FIG. **11**. This provides a saturation transform in which the spectral content of the attenuated energy is examined by looking at every possible saturation value and examining the output value for the assumed saturation value. As will be understood, where the inputs to the multi-variate process estimator **531** are mostly correlated, the sum of squares for the corresponding output vector of the multi-variate process estimator **531** will be very low. Conversely, where the correlation between the first and second inputs to the multi-variate process estimator **531** are not significantly correlated, the sum of squares of the output vector will be high. Accordingly, where the spectral content of the reference signal and the first input to the multi-variate process estimator **531** are made up mostly of physiological (e.g., movement of venous blood due to respiration) and non-physiological (e.g., motion induced) noise, the output energy will be low. Where the spectral content of the reference signal and the first input to the multi-variate process estimator **531** are not correlated, the output energy will be much higher.

[0110] A corresponding transform is completed by the Bin Power Curves module **558**, except a saturation transform power curve is generated for each bin. The resulting power curves are provided as the outputs of the saturation transform module **406**.

[0111] In general, in accordance with the signal model embodiment of the present invention, there will be two peaks in the power curves, as depicted in FIG. **11**. One peak corresponds to the arterial oxygen saturation of the blood, and one peak corresponds to the venous oxygen concentration of the blood. With reference to the signal model of the present invention, the peak corresponding to the highest saturation value (not necessarily the peak with the greatest magnitude) corresponds to the proportionality coefficient r_a. In other words, the proportionality coefficient r_a corresponds to the ratio which will be measured for the arterial saturation. Similarly, peak that corresponds to the lowest saturation value (not necessarily the peak with the lowest magnitude) will generally correspond to the venous oxygen saturation, which corresponds to the proportionality coefficient r_v in the signal model of the present invention. Therefore, the proportionality coefficient r_v will be a ratio corresponding to the venous oxygen saturation.

[0112] In order to obtain arterial oxygen saturation, the peak in the power curves corresponding to the highest saturation value could be selected. However, to improve confidence in the value, further processing is completed. FIG. **12** illustrates the operation of the saturation calculation module **408** based upon the output of the saturation transform module **406** and the output of the statistics module **404**. As depicted in FIG. **12**, the bin power curves and the bin statistics are provided to the saturation calculation module **408**. In the present embodiment, the master power curves are not provided to the saturation module **408** but can be displayed for a visual check on system operation. The bin statistics contain the normalized RMS values for each of the wavelengths signals, the seed saturation value, and a value representing the cross-correlation between the various wavelengths's signals, as described in greater detail above with respect to the statistics module **404** of FIG. **9**.

[0113] The saturation calculation module **408** first determines a plurality of bin attributes as represented by the compute bin attributes module **560**. The compute bin attributes module **560** collects a data bin from the information from the bin power curves and the information from the bin statistics. In the present embodiment, this operation involves placing the saturation value of the peak from each power curve corresponding to the highest saturation value in the data bin. In the present embodiment, the selection of the highest peak is performed by first computing the first derivative of the power curve in question by convolving the power curve with a smoothing differentiator filter function. In the present embodiment, the smoothing differentiator filter function (using a FIR filter) has the following coefficients:

0.014964670230367

0.098294046682706

0.204468276324813

2.717182664241813

5.704485606695227

0.000000000000000

−5.704482606695227

−2.717182664241813

−0.204468276324813

−0.098294046682706

−0.014964670230367

[0114] This filter performs the differentiation and smoothing. Next, each point in the original power curve in question is evaluated and determined to be a possible peak if the following conditions are met: (1) the point is at least 2% of the maximum value in the power curve; and (2) the value of the first derivative changes from greater than zero to less than or equal to zero. For each point that is found to be a possible peak, the neighboring points are examined and the largest of the three points is considered to be the true peak.

[0115] The peak width for these selected peaks is also calculated. The peak width of a power curve in question is computed by summing all the points in the power curve and subtracting the product of the minimum value in the power curve and the number of points in the power curve. In the present embodiment, the peak width calculation is applied to each of the bin power curves. The maximum value is selected as the peak width.

[0116] In addition, the RMS value from the entire snapshot, the individual wavelengths's RMS values, the seed saturation value for each bin, and the cross correlation between the n wavelengths's signals from the statistics module **404** are also placed in the data bin. The attributes are then used to determine whether the data bin consists of acceptable data, as represented in a bin qualifying logic module **562**.

[0117] If the correlation is too low, the bin is discarded. If the saturation value of the selected peak for a given bin is lower than the seed saturation for the same bin, the peak is replaced with the seed saturation value. If any wavelength's RMS value is below a threshold, the bins are all discarded, and no saturation value is provided, because the measured signals are considered to be too small to obtain meaningful data. If no bins contain acceptable data, the exception handling module **563** provides a message to the display **336** that the data is erroneous.

[0118] If some bins qualify, those bins that qualify as having acceptable data are selected, and those that do not qualify are replaced with the average of the bins that are accepted. Each bin is given a time stamp in order to maintain the time sequence. A voter operation **565** examines each of the bins and selects the three highest saturation values. These values are forwarded to a clip and smooth operation **566**.

[0119] The clip and smooth operation **566** performs averaging with a low pass filter. The low pass filter provides adjustable smoothing as selected by a select smoothing filter module **568**. The select smoothing filter module **568** performs its operation based upon a confidence determination performed by a high confidence test module **570**. The high confidence test is an examination of the peak width for the bin power curves. The width of the peaks provides some indication of motion by the patient, wherein wider peaks indicate motion. Therefore, if the peaks are wide, the smoothing filter is slowed down. If peaks are narrow, the smoothing filter speed is increased. Accordingly, the smoothing filter **566** is adjusted based on the confidence level. The output of the clip and smooth module **566** provides the oxygen saturation values in accordance with one embodiment of the present invention.

[0120] In one embodiment, the clip and smooth filter **566** takes each new saturation value and compares it to the current

saturation value. If the magnitude of the difference is less than 16 (percent oxygen saturation) then the value is pass. Otherwise, if the new saturation value is less than the filtered saturation value, the new saturation value is changed to 16 less than the filtered saturation value. If the new saturation value is greater than the filtered saturation value, then the new saturation value is changed to 16 more than the filtered saturation value.

[0121] During high confidence (no motion), the smoothing filter is a simple one-pole or exponential smoothing filter which in one embodiment is computed as follows:

$$y(n)=0.6*x(n)+0.4*y(n-1)$$

where x(n) is the clipped new saturation value, and y(n) is the filtered saturation value.

[0122] During motion condition, a three-pole infinite impulse response (IIR) filter is used. Its characteristics are controlled by three time constants t_a, t_b, and t_c with values of 0.985, 0.900, and 0.94 respectively. The coefficients for a direct form I, BR filter are computed from these time constants using the following relationships:

$$a_0=0$$

$$a_1=t_b+(t_c)(t_a+t_b)$$

$$a_2=(-t_b)(t_c)(t_a+t_b+(t_c)(t_a))$$

$$a_3=(t_b)^2(t_c)^2(t_a)$$

$$b_0=1-t_b-(t_c)(t_a+(t_c)(t_b))$$

$$b_1=2(t_b)(t_c)(t_a-1)$$

$$b_2=(t_b)(t_c)(t_b+(t_c)(t_a)-(t_b)(t_c)(t_a)-t_a)$$

[0123] It is well understood by those of skill in the art that the normalized plethysmographic waveforms of the multi-wavelength physiological monitor may be utilized to determine the pulse rate of the patient. For example, in one embodiment, the normalized plethysmographic waveforms of the multi-wavelength physiological monitor, illustrated as lines λ_1 RMS, λ_2 RMS, . . . λ_n RMS in FIG. **9**, or the outputs **542** of FIG. **10** may be used to determine the patient's pulse rate. In one embodiment, a Fourier transform is performed on at least one of the normalized plethysmographic waveforms to convert the data of the waveform from the time domain into the frequency domain using methods well known to those of skill in the art. In one embodiment, the first harmonic of the frequency data is identified as the patient's pulse rate.

[0124] Other methods of determining pulse rate or heart rate from normalized plethysmographic data is disclosed in U.S. Pat. No. 5,632,272, incorporated by reference in its entirety herein.

[0125] While a number of preferred embodiments of the invention and variations thereof have been described in detail, other modifications and methods of using and medical applications for the same will be apparent to those of skill in the art. Accordingly, it should be understood that various applications, modifications, and substitutions may be made of equivalents without departing from the spirit of the invention or the scope of the claims.

What is claimed is:

1. A physiological monitor for determining blood oxygen saturation of a patient, the physiological monitor comprising:
- a pulse oximetry sensor, wherein the pulse oximetry sensor comprises:
  - three or more light emitting diodes, wherein each light emitting diode is operative to emit light of a different wavelength; and
  - a detector adapted to receive light from the at least three light emitting diodes after being attenuated by tissue of a medical patient, wherein the detector provides an output signal based at least in part upon the received light; and
- a processor configured to compute a ratio based at least in part on three or more plethysmographic signals obtained from the output signal, the processor further configured to determine the blood oxygen saturation of said medical patient based upon said ratio and one or more blood constituents identified from said output signal.

2. The physiological monitor of claim **1**, wherein the processor is further configured to determine the blood oxygen saturation of said medical patient by compensating the blood oxygen saturation with data regarding the one or more blood constituents.

3. The physiological monitor of claim **1**, wherein the ratio comprises a quotient of a first value and a second value, wherein:
- the first value comprises a first sum of first electrical signals corresponding to the three or more light emitting diodes, the first electrical signals multiplied by a first set of vector coefficients; and
- the second value comprises a second sum of second electrical signals corresponding to the three or more light emitting diodes, the second electrical signals multiplied by a second set of vector coefficients.

4. The physiological monitor of claim **3**, wherein the first and second sets of vector coefficients are determined based upon calibration data.

5. The physiological monitor of claim **3**, wherein the first and second sets of vector coefficients are determined based upon fitting of experimental data.

6. The physiological monitor of claim **1**, wherein the ratio is substantially linear over a range of ratio values, wherein the range of ratio values comprises from about 0.45 to about 1.6.

7. The physiological monitor of claim **1**, wherein the ratio is substantially linear over a range of blood oxygen saturation values, wherein the range of blood oxygen saturation values comprises from about 75% to about 95%.

8. The physiological monitor of claim **1**, wherein the blood constituent comprises methemoglobin.

9. The physiological monitor of claim **1**, wherein the blood constituent comprises carboxyhemoglobin.

10. The physiological monitor of claim **1**, wherein the blood constituent comprises a low hemoglobin level.

11. The physiological monitor of claim **1**, wherein the blood constituent comprises a high hemoglobin level.

12. The physiological monitor of claim **1**, wherein the blood constituent comprises bilirubin.

13. The physiological monitor of claim **1**, wherein the blood constituent comprises methylene blue.

14. The physiological monitor of claim **1**, wherein the blood constituent comprises deoxyhemoglobin.

15. The physiological monitor of claim **1**, wherein the blood constituent comprises lipids.

16. The physiological monitor of claim **1**, wherein the ratio is configured to have reduced tolerance at lower blood oxygen saturation levels compared to a two wavelength blood oxygen saturation system.

17. A physiological monitor sensor comprising:

three or more emitters configured to transmit light through a tissue site of a medical patient; and

at least one detector configured to:

measure the light transmitted through the tissue site of the medical patient by the three or more emitters; and

generate at least one signal configured to be used by a processor to compute a ratio based at least in part on the at least one signal, the processor further configured to determine the blood oxygen saturation of said medical patient based upon said ratio and one or more blood constituents identified from said signal.

18. The sensor of claim **17**, wherein the sensor is capable of removable attachment to the tissue site of the medical patient.

19. The sensor of claim **17**, wherein the three or more emitters comprise eight emitters.

20. The sensor of claim **17**, wherein the ratio is substantially linear over a range of blood oxygen saturation values, wherein the range of blood oxygen saturation values comprises from about 75% to about 95%.

21. The sensor of claim **17**, wherein a blood oxygen saturation of the medical patient calculated based at least in part on the ratio is configured to exhibit higher accuracy at lower blood oxygen saturation levels compared to a two wavelength blood oxygen saturation system.

22. The sensor of claim **17**, wherein the one or more blood constituents comprises one or more of the following:

methemoglobin, carboxyhemoglobin, a low hemoglobin level, a high hemoglobin level, bilirubin, methylene blue, deoxyhemoglobin, or lipids.

23. A method of determining the blood oxygen saturation of a patient, the method comprising:

receiving at least three photoplethysmographic signals indicative of at least three wavelengths of light that have been attenuated by tissue;

determining at least three output signals based upon the at least three photoplethysmographic signals;

calculating a ratio based at least in part on the at least three output signals; and

determining a blood oxygen saturation based at least in part on the ratio and one or more blood constituents identified from said at least three photoplethysmographic signals.

24. The method of claim **23**, wherein the ratio exhibits greater linearity over a first range of ratio values compared to a linearity over a second range of ratio values in a two-wavelength blood oxygen saturation system.

25. The method of claim **23**, further comprising selecting a data signal corresponding to attenuated light from one of the at least three photoplethysmographic signals.

26. The method of claim **25**, further comprising providing a process estimator output using a multi-variate process estimator based at least in part upon the ratio and the selected data signal, such that a blood oxygen saturation of a patient may be calculated in response to the process estimator output.

27. The method of claim **26**, wherein the multi-variate process estimator comprises a pseudo-inverse.

28. The method of claim **23**, wherein the one or more blood constituents comprises one or more of the following:

methemoglobin, carboxyhemoglobin, a low hemoglobin level, a high hemoglobin level, bilirubin, methylene blue, deoxyhemoglobin, or lipids.

* * * * *